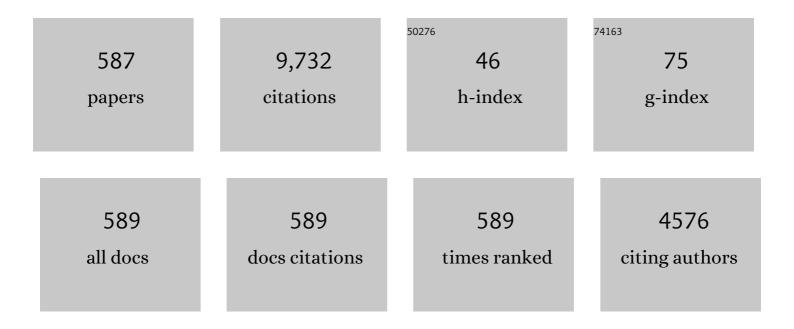
List of Publications by Year in descending order

Source: https://exaly.com/author-pdf/2682965/publications.pdf Version: 2024-02-01



#	Article	IF	CITATIONS
1	A quantum-dot spin qubit with coherence limited by charge noise and fidelity higher than 99.9%. Nature Nanotechnology, 2018, 13, 102-106.	31.5	574
2	Optical properties of ZnO rods formed by metalorganic chemical vapor deposition. Applied Physics Letters, 2003, 83, 1635-1637.	3.3	319
3	Island formation during growth of Ge on Si(100): A study using photoluminescence spectroscopy. Applied Physics Letters, 1995, 66, 3024-3026.	3.3	263
4	Formation of highly aligned ZnO tubes on sapphire (0001) substrates. Applied Physics Letters, 2004, 84, 4098-4100.	3.3	183
5	Growth of structure-controlled polycrystalline silicon ingots for solar cells by casting. Acta Materialia, 2006, 54, 3191-3197.	7.9	158
6	Investigation of grain boundaries in BaSi2 epitaxial films on Si(1 1 1) substrates using transmission electron microscopy and electron-beam-induced current technique. Journal of Crystal Growth, 2012, 348, 75-79.	1.5	133
7	Control of Ge dots in dimension and position by selective epitaxial growth and their optical properties. Applied Physics Letters, 1998, 72, 1617-1619.	3.3	128
8	Effects of growth temperature on the characteristics of ZnO epitaxial films deposited by metalorganic chemical vapor deposition. Thin Solid Films, 2004, 449, 12-19.	1.8	112
9	Growth of ZnOâ^•MgZnO quantum wells on sapphire substrates and observation of the two-dimensional confinement effect. Applied Physics Letters, 2005, 86, 032105.	3.3	112
10	Grain growth behaviors of polycrystalline silicon during melt growth processes. Journal of Crystal Growth, 2004, 266, 441-448.	1.5	101
11	Directional growth method to obtain high quality polycrystalline silicon from its melt. Journal of Crystal Growth, 2006, 292, 282-285.	1.5	100
12	Enhanced quantum efficiency of solar cells with self-assembled Ge dots stacked in multilayer structure. Applied Physics Letters, 2003, 83, 1258-1260.	3.3	99
13	Exploring the potential of semiconducting BaSi ₂ for thin-film solar cell applications. Journal Physics D: Applied Physics, 2017, 50, 023001.	2.8	99
14	In situ observation of elementary growth steps on the surface of protein crystals by laser confocal microscopy. Journal of Crystal Growth, 2004, 262, 536-542.	1.5	98
15	Generation mechanism of dislocations during directional solidification of multicrystalline silicon using artificially designed seed. Journal of Crystal Growth, 2010, 312, 897-901.	1.5	96
16	Low-temperature (180 °C) formation of large-grained Ge (111) thin film on insulator using accelerated metal-induced crystallization. Applied Physics Letters, 2014, 104, .	3.3	96
17	Highly (111)-oriented Ge thin films on insulators formed by Al-induced crystallization. Applied Physics Letters, 2012, 101, 072106.	3.3	88
18	Investigation of the recombination mechanism of excess carriers in undoped BaSi2 films on silicon. Journal of Applied Physics, 2012, 112, .	2.5	84

#	Article	IF	CITATIONS
19	In situ observation of Si faceted dendrite growth from low-degree-of-undercooling melts. Acta Materialia, 2008, 56, 2663-2668.	7.9	82
20	Influence of grain size and surface condition on minority-carrier lifetime in undoped <i>n</i> -BaSi2 on Si(111). Journal of Applied Physics, 2014, 115, .	2.5	80
21	Strong resonant luminescence from Ge quantum dots in photonic crystal microcavity at room temperature. Applied Physics Letters, 2006, 89, 201102.	3.3	79
22	Determination of Bulk Minority-Carrier Lifetime in BaSi ₂ Earth-Abundant Absorber Films by Utilizing a Drastic Enhancement of Carrier Lifetime by Post-Growth Annealing. Applied Physics Express, 2013, 6, 112302.	2.4	75
23	Optical anisotropy in wireâ€geometry SiGe layers grown by gasâ€source selective epitaxial growth technique. Applied Physics Letters, 1994, 64, 1126-1128.	3.3	74
24	Formation mechanism of parallel twins related to Si-facetted dendrite growth. Scripta Materialia, 2007, 57, 81-84.	5.2	74
25	<i>In-situ</i> heavily <i>p</i> -type doping of over 1020 cmâ^'3 in semiconducting BaSi2 thin films for solar cells applications. Applied Physics Letters, 2013, 102, .	3.3	72
26	In situ observations of crystal growth behavior of silicon melt. Journal of Crystal Growth, 2002, 243, 275-282.	1.5	71
27	In-situ observations of melt growth behavior of polycrystalline silicon. Journal of Crystal Growth, 2004, 262, 124-129.	1.5	69
28	p-BaSi2/n-Si heterojunction solar cells with conversion efficiency reaching 9.0%. Applied Physics Letters, 2016, 108, .	3.3	69
29	Growth Mechanism of Si-Faceted Dendrites. Physical Review Letters, 2008, 101, 055503.	7.8	66
30	Investigation of the open-circuit voltage in solar cells doped with quantum dots. Scientific Reports, 2013, 3, 2703.	3.3	65
31	In-plane strain fluctuation in strained-Si/SiGe heterostructures. Applied Physics Letters, 2003, 83, 4339-4341.	3.3	61
32	Molecular beam epitaxy of BaSi2 thin films on Si(001) substrates. Journal of Crystal Growth, 2012, 345, 16-21.	1.5	61
33	Photoresponse Properties of Polycrystalline BaSi ₂ Films Grown on SiO ₂ Substrates Using (111)-Oriented Si Layers by an Aluminum-Induced Crystallization Method. Applied Physics Express, 0, 2, 051601.	2.4	55
34	Abrupt Si/Ge interface formation using atomic hydrogen in Si molecular beam epitaxy. Applied Physics Letters, 1994, 65, 2975-2977.	3.3	54
35	Room-temperature electroluminescence from Si microdisks with Ge quantum dots. Optics Express, 2010, 18, 13945.	3.4	54
36	Luminescence study on interdiffusion in strained Si1â^'xGex/Si single quantum wells grown by molecular beam epitaxy. Applied Physics Letters, 1993, 63, 1651-1653.	3.3	53

#	Article	IF	CITATIONS
37	Realization of crescentâ€shaped SiGe quantum wire structures on a Vâ€groove patterned Si substrate by gasâ€source Si molecular beam epitaxy. Applied Physics Letters, 1993, 63, 2789-2791.	3.3	53
38	Pressure-Dependent ZnO Nanocrsytal Growth in a Chemical Vapor Deposition Process. Journal of Physical Chemistry B, 2004, 108, 10899-10902.	2.6	52
39	Formation mechanism of a faceted interface: <i>In situ</i> observation of the Si(100) crystal-melt interface during crystal growth. Physical Review B, 2009, 80, .	3.2	52
40	Improved photoresponsivity of semiconducting BaSi ₂ epitaxial films grown on a tunnel junction for thin-film solar cells. Applied Physics Letters, 2012, 100, 152114.	3.3	50
41	Control of Grain Boundary Propagation in Mono-Like Si: Utilization of Functional Grain Boundaries. Applied Physics Express, 2013, 6, 025505.	2.4	50
42	Dislocation glide motion in heteroepitaxial thin films of Si _{1â^'x} Ge _x /Si(100). Philosophical Magazine Letters, 1993, 67, 165-171.	1.2	49
43	Growth of SiGe bulk crystal with uniform composition by directly controlling the growth temperature at the crystal–melt interface using in situ monitoring system. Journal of Crystal Growth, 2001, 224, 204-211.	1.5	49
44	Analysis of the electrical properties of Cr/n-BaSi2 Schottky junction and n-BaSi2/p-Si heterojunction diodes for solar cell applications. Journal of Applied Physics, 2014, 115, .	2.5	49
45	Mono-Like Silicon Growth Using Functional Grain Boundaries to Limit Area of Multicrystalline Grains. IEEE Journal of Photovoltaics, 2014, 4, 84-87.	2.5	48
46	Observation of deepâ€levelâ€free band edge luminescence and quantum confinement in strained Si1â^'xGex/Si single quantum well structures grown by solid source Si molecular beam epitaxy. Applied Physics Letters, 1992, 61, 1706-1708.	3.3	47
47	Temperature dependence of microscopic photoluminescence spectra of quantum dots and quantum wells. Physica E: Low-Dimensional Systems and Nanostructures, 1998, 2, 573-577.	2.7	47
48	Gas-source molecular beam epitaxy and luminescence characterization of strained Silâ^'xGex/Si quantum wells. Journal of Crystal Growth, 1994, 136, 315-321.	1.5	46
49	Enhancement of radiative recombination in Siâ€based quantum wells with neighboring confinement structure. Applied Physics Letters, 1995, 67, 524-526.	3.3	46
50	Low-temperature growth of ZnO nanostructure networks. Journal of Applied Physics, 2004, 96, 340-343.	2.5	46
51	Relationship between grain boundary structures in Si multicrystals and generation of dislocations during crystal growth. Journal of Applied Physics, 2010, 107, .	2.5	46
52	Photoluminescence investigation on growth mode changeover of Ge on Si(100). Journal of Crystal Growth, 1995, 157, 265-269.	1.5	45
53	Orientation Control of Large-Grained Si Films on Insulators by Thickness-Modulated Al-Induced Crystallization. Crystal Growth and Design, 2013, 13, 1767-1770.	3.0	44
54	Fabrication of high-quality strain-relaxed thin SiGe layers on ion-implanted Si substrates. Applied Physics Letters, 2004, 85, 2514-2516.	3.3	43

#	Article	IF	CITATIONS
55	Enhanced carrier extraction from Ge quantum dots in Si solar cells under strong photoexcitation. Applied Physics Letters, 2012, 101, .	3.3	43
56	Silicon-based light emitters fabricated by embedding Ge self-assembled quantum dots in microdisks. Applied Physics Letters, 2007, 91, .	3.3	42
57	Growth of multicrystalline Si ingots using noncontact crucible method for reduction of stress. Journal of Crystal Growth, 2012, 344, 6-11.	1.5	42
58	Configuration and local elastic interaction of ferroelectric domains and misfit dislocation in PbTiO ₃ /SrTiO ₃ epitaxial thin films. Science and Technology of Advanced Materials, 2011, 12, 034413.	6.1	41
59	Realization of single-phase BaSi ₂ films by vacuum evaporation with suitable optical properties and carrier lifetime for solar cell applications. Japanese Journal of Applied Physics, 2015, 54, 07JE02.	1.5	41
60	Observation of lateral confinement effect in Ge quantum wires selfâ€aligned at step edges on Si(100). Applied Physics Letters, 1996, 68, 1847-1849.	3.3	40
61	Selective formation of large-grained, (100)- or (111)-oriented Si on glass by Al-induced layer exchange. Journal of Applied Physics, 2014, 115, .	2.5	40
62	Microstructures of Si multicrystals and their impact on minority carrier diffusion length. Acta Materialia, 2009, 57, 3268-3276.	7.9	39
63	Luminescence from Strained Si1-xGex/Si Quantum Wells Grown by Si Molecular Beam Epitaxy. Japanese Journal of Applied Physics, 1993, 32, 1502-1507.	1.5	38
64	Seed manipulation for artificially controlled defect technique in new growth method for quasi-monocrystalline Si ingot based on casting. Applied Physics Express, 2015, 8, 105501.	2.4	38
65	Simultaneous enhanced photon capture and carrier generation in Si solar cells using Ge quantum dot photonic nanocrystals. Nanotechnology, 2012, 23, 185401.	2.6	36
66	Bandâ€edge photoluminescence of SiGe/strained‣i/SiGe typeâ€II quantum wells on Si(100). Applied Physics Letters, 1993, 63, 3509-3511.	3.3	35
67	Compositional variation in Si-rich SiGe single crystals grown by multi-component zone melting method using Si seed and source crystals. Journal of Crystal Growth, 2002, 240, 373-381.	1.5	35
68	Floating cast method to realize high-quality Si bulk multicrystals for solar cells. Journal of Crystal Growth, 2009, 311, 228-231.	1.5	35
69	Epitaxial Growth and Polarity of ZnO Films on Sapphire (0001) Substrates by Low-Pressure Metal Organic Chemical Vapor Deposition. Japanese Journal of Applied Physics, 2003, 42, 2291-2295.	1.5	34
70	Highâ€ŧemperature operation of strained Si0.65Ge0.35/Si(111)pâ€ŧype multipleâ€quantumâ€well lightâ€emitti diode grown by solid source Si molecularâ€beam epitaxy. Applied Physics Letters, 1993, 63, 967-969.	۱g _{3.3}	33
71	Fabrication of n ⁺ -BaSi ₂ /p ⁺ -Si Tunnel Junction on Si(111) Surface by Molecular Beam Epitaxy for Photovoltaic Applications. Applied Physics Express, 2010, 3, 021301.	2.4	33
72	Electroluminescence from Strained SiGe/Si Quantum Well Structures Grown by Solid Source Si Molecular Beam Epitaxy. Japanese Journal of Applied Physics, 1992, 31, L1015-L1017.	1.5	32

#	Article	IF	CITATIONS
73	Ge composition dependence of properties of solar cells based on multicrystalline SiGe with microscopic compositional distribution. Journal of Applied Physics, 2004, 96, 1238-1241.	2.5	32
74	Precipitation control and activation enhancement in boron-doped p <i>+</i> -BaSi2 films grown by molecular beam epitaxy. Applied Physics Letters, 2014, 104, .	3.3	32
75	Fabrication and characterization of BaSi ₂ epitaxial films over 1 µm in thickness on Si(111). Japanese Journal of Applied Physics, 2014, 53, 04ER04.	1.5	31
76	Fabrication of single-phase polycrystalline BaSi ₂ thin films on silicon substrates by vacuum evaporation for solar cell applications. Japanese Journal of Applied Physics, 2015, 54, 08KC03.	1.5	31
77	Structural and electrical characterizations of crack-free BaSi2 thin films fabricated by thermal evaporation. Thin Solid Films, 2015, 595, 68-72.	1.8	31
78	Optimized electrical control of a Si/SiGe spin qubit in the presence of an induced frequency shift. Npj Quantum Information, 2018, 4, .	6.7	31
79	Growth of SiGe bulk crystals with uniform composition by utilizing feedback control system of the crystal–melt interface position for precise control of the growth temperature. Journal of Crystal Growth, 2003, 250, 298-304.	1.5	30
80	Growth of multicrystalline Si with controlled grain boundary configuration by the floating zone technique. Journal of Crystal Growth, 2005, 280, 419-424.	1.5	30
81	On the Controlling Mechanism of Preferential Orientation of Polycrystalline-Silicon Thin Films Grown by Aluminum-Induced Crystallization. Applied Physics Express, 2010, 3, 095803.	2.4	30
82	Quantum Size Effect of Excitonic Band-Edge Luminescence in Strained Si1-xGex/Si Single Quantum Well Structures Grown by Gas-Source Si Molecular Beam Epitaxy. Japanese Journal of Applied Physics, 1992, 31, L1319-L1321.	1.5	29
83	Abrupt compositional transition in luminescent Si1â^'xGex/Si quantum well structures fabricated by segregant assisted growth using Sb adlayer. Applied Physics Letters, 1993, 63, 388-390.	3.3	29
84	High-Quality Polycrystalline Silicon Films with Minority Carrier Lifetimes over 5 µs Formed by Flash Lamp Annealing of Precursor Amorphous Silicon Films Prepared by Catalytic Chemical Vapor Deposition. Japanese Journal of Applied Physics, 2007, 46, 7198.	1.5	29
85	Fabrication of (111)-oriented Si layers on SiO2 substrates by an aluminum-induced crystallization method and subsequent growth of semiconducting BaSi2 layers for photovoltaic application. Journal of Crystal Growth, 2009, 311, 3581-3586.	1.5	29
86	Evaluation of potential variations around grain boundaries in BaSi2 epitaxial films by Kelvin probe force microscopy. Applied Physics Letters, 2013, 103, .	3.3	29
87	Formation of metastable cubic phase in SnS thin films fabricated by thermal evaporation. Thin Solid Films, 2017, 639, 7-11.	1.8	29
88	Simple method for significant improvement of minority-carrier lifetime of evaporated BaSi 2 thin film by sputtered-AlO x passivation. Materials Science in Semiconductor Processing, 2018, 76, 37-41.	4.0	29
89	Silicon-Based Light-Emitting Devices Based on Ge Self-Assembled Quantum Dots Embedded in Optical Cavities. IEEE Journal of Selected Topics in Quantum Electronics, 2012, 18, 1830-1838.	2.9	28
90	Effects of deposition rate on the structure and electron density of evaporated BaSi2 films. Journal of Applied Physics, 2016, 120, 045103.	2.5	28

#	Article	IF	CITATIONS
91	Silicon–germanium (SiGe) nanostructures. , 2011, , .		28
92	Selective epitaxial growth of dot structures on patterned Si substrates by gas source molecular beam epitaxy. Semiconductor Science and Technology, 1999, 14, 257-265.	2.0	27
93	Crystal quality of a 6H-SiC layer grown over macrodefects by liquid-phase epitaxy: a Raman spectroscopic study. Thin Solid Films, 2005, 476, 206-209.	1.8	27
94	Quantitative analysis of subgrain boundaries in Si multicrystals and their impact on electrical properties and solar cell performance. Journal of Applied Physics, 2009, 105, 044909.	2.5	27
95	Formation mechanism of twin boundaries during crystal growth of silicon. Scripta Materialia, 2011, 65, 556-559.	5.2	27
96	Hydrogen concentration at a-Si:H/c-Si heterointerfaces—The impact of deposition temperature on passivation performance. AIP Advances, 2019, 9, .	1.3	27
97	Role of heterointerface on enhancement of noâ€phonon luminescence in Siâ€based neighboring confinement structure. Applied Physics Letters, 1996, 68, 2340-2342.	3.3	26
98	Raman scattering and x-ray absorption studies of Ge–Si nanocrystallization. Applied Physics Letters, 2002, 80, 488-490.	3.3	26
99	Floating zone growth of Si-rich SiGe bulk crystal using pre-synthesized SiGe feed rod with uniform composition. Journal of Crystal Growth, 2005, 284, 57-64.	1.5	26
100	Growth mechanism of the Si⟠110⟠©faceted dendrite. Physical Review B, 2010, 81, .	3.2	26
101	N-type doping of BaSi2 epitaxial films by phosphorus ion implantation and thermal annealing. Thin Solid Films, 2014, 557, 90-93.	1.8	26
102	Postannealing effects on undoped BaSi ₂ evaporated films grown on Si substrates. Japanese Journal of Applied Physics, 2017, 56, 05DB05.	1.5	25
103	Drastic modification of the growth mode of Ge quantum dots on Si by using boron adlayer. Thin Solid Films, 2000, 369, 84-87.	1.8	23
104	Generation mechanism of dislocations and their clusters in multicrystalline silicon during two-dimensional growth. Journal of Applied Physics, 2011, 110, 083530.	2.5	23
105	Upper limit of two-dimensional hole gas mobility in strained Ge/SiGe heterostructures. Applied Physics Letters, 2012, 100, .	3.3	23
106	Potential variations around grain boundaries in impurity-doped BaSi2 epitaxial films evaluated by Kelvin probe force microscopy. Journal of Applied Physics, 2014, 116, .	2.5	23
107	Optical investigation of modified Stranski–Krastanov growth mode in the stacking of self-assembled Ge islands. Thin Solid Films, 2000, 369, 108-111.	1.8	22
108	Effects of high pressure on the growth kinetics of orthorhombic lysozyme crystals. Journal of Crystal Growth, 2003, 254, 188-195.	1.5	22

#	Article	IF	CITATIONS
109	Effects of spacer thickness on quantum efficiency of the solar cells with embedded Ge islands in the intrinsic layer. Applied Physics Letters, 2004, 84, 2802-2804.	3.3	22
110	Strain dependence of hole effective mass and scattering mechanism in strained Ge channel structures. Applied Physics Letters, 2009, 95, .	3.3	22
111	Impact of type of crystal defects in multicrystalline Si on electrical properties and interaction with impurities. Journal of Applied Physics, 2011, 109, .	2.5	22
112	N-type doping of BaSi2 epitaxial films by arsenic ion implantation through a dose-dependent carrier generation mechanism. Thin Solid Films, 2014, 567, 105-108.	1.8	22
113	On the origin of strain fluctuation in strained-Si grown on SiGe-on-insulator and SiGe virtual substrates. Applied Physics Letters, 2004, 85, 1335-1337.	3.3	21
114	Determination of lattice parameters of SiGe/Si(110) heterostructures. Thin Solid Films, 2006, 508, 132-135.	1.8	21
115	Silicon-based current-injected light emitting diodes with Ge self-assembled quantum dots embedded in photonic crystal nanocavities. Optics Express, 2012, 20, 14714.	3.4	21
116	Dependence of crystal orientation in Al-induced crystallized poly-Si layers on SiO2 insertion layer thickness. Journal of Crystal Growth, 2012, 356, 65-69.	1.5	21
117	Lattice and grain-boundary diffusions of boron atoms in BaSi2 epitaxial films on Si(111). Journal of Applied Physics, 2013, 113, .	2.5	21
118	Enhancement of light emission from Ge quantum dots by photonic crystal nanocavities at room-temperature. Journal of Crystal Growth, 2013, 378, 636-639.	1.5	21
119	Effects of crystal defects and their interactions with impurities on electrical properties of multicrystalline Si. Journal of Applied Physics, 2013, 113, 133503.	2.5	21
120	Photoresponse properties of BaSi ₂ film grown on Si (100) by vacuum evaporation. Materials Research Express, 2016, 3, 076204.	1.6	21
121	On the Mechanism of BaSi2 Thin Film Formation on Si Substrate by Vacuum Evaporation. Procedia Engineering, 2016, 141, 23-26.	1.2	21
122	Is low temperature growth the solution to abrupt Siâ§,Si1-xGex interface formation?. Journal of Crystal Growth, 1993, 127, 401-405.	1.5	20
123	Ultrashort lifetime photocarriers in Ge thin films. Applied Physics Letters, 1996, 68, 3419-3421.	3.3	20
124	Epitaxial relation and island growth of perylene-3.4.9.10-tetracarboxylic dianhydride (PTCDA) thin film crystals on a hydrogen-terminated Si(111) substrate. Journal of Crystal Growth, 2004, 262, 196-201.	1.5	20
125	Influence of structural imperfection of Σ5 grain boundaries in bulk multicrystalline Si on their electrical activities. Journal of Applied Physics, 2007, 101, 063509.	2.5	20
126	Acceptorlike Behavior of Defects in SiGe Alloys Grown by Molecular Beam Epitaxy. Japanese Journal of Applied Physics, 2008, 47, 4630.	1.5	20

#	Article	IF	CITATIONS
127	Implementation of faceted dendrite growth on floating cast method to realize high-quality multicrsytalline Si ingot for solar cells. Journal of Applied Physics, 2011, 109, .	2.5	20
128	Effects of formation of mini-bands in two-dimensional array of silicon nanodisks with SiC interlayer for quantum dot solar cells. Nanotechnology, 2013, 24, 015301.	2.6	20
129	Evaluation of minority carrier diffusion length of undoped n-BaSi ₂ epitaxial thin films on Si(001) substrates by electron-beam-induced-current technique. Japanese Journal of Applied Physics, 2014, 53, 078004.	1.5	20
130	Formation process of Si3N4 particles on surface of Si ingots grown using silica crucibles with Si3N4 coating by noncontact crucible method. Journal of Crystal Growth, 2014, 389, 112-119.	1.5	20
131	Impact of silicon quantum dot super lattice and quantum well structure as intermediate layer on pâ€iâ€n silicon solar cells. Progress in Photovoltaics: Research and Applications, 2016, 24, 774-780.	8.1	20
132	Simple Vacuum Evaporation Route to BaSi2 Thin Films for Solar Cell Applications. Procedia Engineering, 2016, 141, 27-31.	1.2	20
133	Marked enhancement of the photoresponsivity and minority-carrier lifetime of <mml:math xmlns:mml="http://www.w3.org/1998/Math/MathML"> <mml:mrow> <mml:mi>BaS</mml:mi> <mml:msub> <mml:r mathvariant="normal">i <mml:mn>2</mml:mn></mml:r </mml:msub> </mml:mrow> passivated with atomic hydrogen. Physical Review Materials. 2019. 3.</mml:math 	ni 2.4	20
134	Growth and characterization of 70 Ge n / 74 Ge n isotope superlattices. Thin Solid Films, 2000, 369, 405-408.	1.8	19
135	Modification of the growth mode of Ge on Si by buried Ge islands. Applied Physics Letters, 2000, 76, 3723-3725.	3.3	19
136	Physical model for the evaluation of solid–liquid interfacial tension in silicon. Journal of Applied Physics, 2001, 90, 750-755.	2.5	19
137	Influence of the elastic strain on the band structure of ellipsoidal SiGe coherently embedded in the Si matrix. Journal of Applied Physics, 2003, 94, 916-920.	2.5	19
138	Theory of open-circuit voltage and the driving force of charge separation in pn-junction solar cells. Journal of Applied Physics, 2013, 114, .	2.5	19
139	Formation of BaSi2 heterojunction solar cells using transparent MoO <i>x</i> hole transport layers. Applied Physics Letters, 2015, 106, .	3.3	19
140	Effects of the Si/Al layer thickness on the continuity, crystalline orientation and the growth kinetics of the poly-Si thin films formed by aluminum-induced crystallization. Thin Solid Films, 2016, 616, 213-219.	1.8	19
141	Formation and optical properties of SiGe/Si quantum structures. Applied Surface Science, 1996, 102, 263-271.	6.1	18
142	Strain-driven alloying: effect on sizes, shape and photoluminescence of GeSi/Si(001) self-assembled islands. Materials Science and Engineering B: Solid-State Materials for Advanced Technology, 2002, 89, 62-65.	3.5	18
143	New method for measurement of interdiffusion coefficient in high temperature solutions based on Fick's first law. Journal of Crystal Growth, 2002, 241, 387-394.	1.5	18
144	Modification of Local Structure and Its Influence on Electrical Activity of Near (310) Σ5 Grain Boundary in Bulk Silicon. Materials Transactions, 2007, 48, 143-147.	1.2	18

#	Article	IF	CITATIONS
145	Molecular Beam Epitaxy of BaSi\$_{2}\$ Films with Grain Size over 4 \$mu\$m on Si(111). Japanese Journal of Applied Physics, 2012, 51, 098003.	1.5	18
146	Molecular beam epitaxy of boron doped p-type BaSi2 epitaxial films on Si(111) substrates for thin-film solar cells. Journal of Crystal Growth, 2013, 378, 201-204.	1.5	18
147	Systematic blue shift of exciton luminescence in strained Si1 â^'s xGex/Si quantum well structures grown by gas source silicon molecular beam epitaxy. Thin Solid Films, 1992, 222, 1-4.	1.8	17
148	Melt growth of multicrystalline SiGe with large compositional distribution for new solar cell applications. Solar Energy Materials and Solar Cells, 2002, 72, 93-100.	6.2	17
149	Magnetotransport properties of Ge channels with extremely high compressive strain. Applied Physics Letters, 2006, 89, 162103.	3.3	17
150	Double-Layered Ge Thin Films on Insulators Formed by an Al-Induced Layer-Exchange Process. Crystal Growth and Design, 2013, 13, 3908-3912.	3.0	17
151	Large-Grained Polycrystalline (111) Ge Films on Insulators by Thickness-Controlled Al-Induced Crystallization. ECS Journal of Solid State Science and Technology, 2013, 2, Q195-Q199.	1.8	17
152	Orientation control of Ge thin films by underlayer-selected Al-induced crystallization. CrystEngComm, 2014, 16, 2578.	2.6	17
153	BaSi ₂ formation mechanism in thermally evaporated films and its application to reducing oxygen impurity concentration. Japanese Journal of Applied Physics, 2018, 57, 04FS01.	1.5	17
154	Reactive deposition growth of highly (001)-oriented BaSi2 films by close-spaced evaporation. Materials Science in Semiconductor Processing, 2020, 113, 105044.	4.0	17
155	Electrical properties of oxides grown on strained Si using microwave N2O plasma. Applied Physics Letters, 1997, 70, 66-68.	3.3	16
156	Formation of relaxed SiGe films on Si by selective epitaxial growth. Thin Solid Films, 2000, 369, 126-129.	1.8	16
157	Growth and properties of SiGe multicrystals with microscopic compositional distribution for high-efficiency solar cells. Solar Energy Materials and Solar Cells, 2002, 73, 305-320.	6.2	16
158	A simple approach to determine preferential growth orientation using multiple seed crystals with random orientations and its utilization for seed optimization to restrain polycrystallization of SiGe bulk crystal. Journal of Crystal Growth, 2005, 276, 393-400.	1.5	16
159	Crystalline morphologies of step-graded SiGe layers grown on exact and vicinal (110) Si substrates. Journal of Crystal Growth, 2009, 311, 809-813.	1.5	16
160	Computational Investigation of Relationship between Shear Stress and Multicrystalline Structure in Silicon. Japanese Journal of Applied Physics, 2010, 49, 04DP01.	1.5	16
161	Temperature dependent Al-induced crystallization of amorphous Ge thin films on SiO2 substrates. Journal of Crystal Growth, 2013, 372, 189-192.	1.5	16
162	Mechanism of strain relaxation in BaSi ₂ epitaxial films on Si(111) substrates during postâ€growth annealing and application for film exfoliation. Physica Status Solidi C: Current Topics in Solid State Physics, 2013, 10, 1677-1680.	0.8	16

#	Article	IF	CITATIONS
163	Growth promotion of Al-induced crystallized Ge films on insulators by insertion of a Ge membrane below the Al layer. Thin Solid Films, 2014, 557, 143-146.	1.8	16
164	Optical characterization of strain-induced structural modification in SiGe-based heterostructures. Journal of Applied Physics, 1999, 85, 2363-2366.	2.5	15
165	SiGe bulk crystal as a lattice-matched substrate to GaAs for solar cell applications. Applied Physics Letters, 2000, 77, 3565-3567.	3.3	15
166	Realization of Bulk Multicrystalline Silicon with Controlled Grain Boundaries by Utilizing Spontaneous Modification of Grain Boundary Configuration. Japanese Journal of Applied Physics, 2006, 45, 1734-1737.	1.5	15
167	Effect of the compositional distribution on the photovoltaic power conversion of SiGe solar cells. Solar Energy Materials and Solar Cells, 2007, 91, 123-128.	6.2	15
168	Growth temperature dependence of lattice structures of SiGe/graded buffer structures grown on Si(110) substrates by gas-source MBE. Journal of Crystal Growth, 2007, 301-302, 343-348.	1.5	15
169	Quantum dot solar cells using 2-dimensional array of 6.4-nm-diameter silicon nanodisks fabricated using bio-templates and neutral beam etching. Applied Physics Letters, 2012, 101, 063121.	3.3	15
170	Epitaxy of Orthorhombic BaSi\$_{2}\$ with Preferential In-Plane Crystal Orientation on Si(001): Effects of Vicinal Substrate and Annealing Temperature. Japanese Journal of Applied Physics, 2012, 51, 095501.	1.5	15
171	Structural study on phosphorus doping of BaSi2 epitaxial films by ion implantation. Thin Solid Films, 2013, 534, 470-473.	1.8	15
172	Fabrication and characterizations of phosphorusâ€doped nâ€ŧype BaSi ₂ epitaxial films grown by molecular beam epitaxy. Physica Status Solidi C: Current Topics in Solid State Physics, 2013, 10, 1753-1755.	0.8	15
173	3D visualization and analysis of dislocation clusters in multicrystalline silicon ingot by approach of data science. Solar Energy Materials and Solar Cells, 2019, 189, 239-244.	6.2	15
174	Local Structure of High Performance TiO <i>_x</i> Electron elective Contact Revealed by Electron Energy Loss Spectroscopy. Advanced Materials Interfaces, 2019, 6, 1801645.	3.7	15
175	Effect of hydrogen plasma treatment on the passivation performance of TiO <i>x</i> on crystalline silicon prepared by atomic layer deposition. Journal of Vacuum Science and Technology A: Vacuum, Surfaces and Films, 2020, 38, .	2.1	15
176	Application of Bayesian optimization for improved passivation performance in TiO _{x } /SiO _y /c-Si heterostructure by hydrogen plasma treatment. Applied Physics Express, 2021, 14, 025503.	2.4	15
177	Fabrication of SiGe/Si quantum wire structures on a V-groove patterned Si substrate by gas-source Si molecular beam epitaxy. Solid-State Electronics, 1994, 37, 539-541.	1.4	14
178	Oxidation of strained Si in a microwave electron cyclotron resonance plasma. Applied Physics Letters, 1997, 70, 217-219.	3.3	14
179	In-situ monitoring system of the position and temperature at the crystal–solution interface. Journal of Crystal Growth, 2002, 236, 125-131.	1.5	14
180	In-Plane Orientation and Polarity of ZnO Epitaxial Films on As-Polished Sapphire (α-Al2O3) (0001) Substrates Grown by Metal Organic Chemical Vapor Deposition. Japanese Journal of Applied Physics, 2003, 42, L264-L266.	1.5	14

#	Article	IF	CITATIONS
181	Structural properties of directionally grown polycrystalline SiGe for solar cells. Journal of Crystal Growth, 2005, 275, 467-473.	1.5	14
182	Structural Origin of a Cluster of Bright Spots in Reverse Bias Electroluminescence Image of Solar Cells Based on Si Multicrystals. Applied Physics Express, 2008, 1, 075001.	2.4	14
183	Strain relaxation mechanisms in step-graded SiGe/Si(110) heterostructures grown by gas-source MBE at high temperatures. Journal of Crystal Growth, 2009, 311, 819-824.	1.5	14
184	Alternative simple method to realize p-type BaSi2 thin films for Si heterojunction solar cell applications. MRS Advances, 2018, 3, 1435-1442.	0.9	14
185	Activation mechanism of TiO <i> _x </i> passivating layer on crystalline Si. Applied Physics Express, 2018, 11, 102301.	2.4	14
186	Application of artificial neural network to optimize sensor positions for accurate monitoring: an example with thermocouples in a crystal growth furnace. Applied Physics Express, 2019, 12, 125503.	2.4	14
187	Hybrid Si molecular beam epitaxial regrowth for a strained Si1â^'xGex/Si singleâ€quantumâ€well electroluminescent device. Applied Physics Letters, 1993, 63, 2414-2416.	3.3	13
188	Anomalous luminescence peak shift of SiGe/Si quantum well induced by self-assembled Ge islands. Applied Physics Letters, 1997, 70, 295-297.	3.3	13
189	Optical investigation of growth mode of Ge thin films on Si(110) substrates. Applied Physics Letters, 1997, 71, 785-787.	3.3	13
190	Stacked Ge islands for photovoltaic applications. Science and Technology of Advanced Materials, 2003, 4, 367-370.	6.1	13
191	Phase diagram of growth mode for the SiGe/Si heterostructure system with misfit dislocations. Journal of Crystal Growth, 2004, 260, 372-383.	1.5	13
192	Step-Induced Anisotropic Growth of Pentacene Thin Film Crystals on a Hydrogen-Terminated Si(111) Surface. Crystal Growth and Design, 2007, 7, 439-444.	3.0	13
193	Introduction of Uniaxial Strain into Si/Ge Heterostructures by Selective Ion Implantation. Applied Physics Express, 0, 1, 121401.	2.4	13
194	Generation and Wavelength Control of Resonant Luminescence from Silicon Photonic Crystal Microcavities with Ge Dots. Japanese Journal of Applied Physics, 2009, 48, 022102.	1.5	13
195	Pattern formation mechanism of a periodically faceted interface during crystallization ofSi. Journal of Crystal Growth, 2010, 312, 3670-3674.	1.5	13
196	Improved multicrystalline silicon ingot quality using single layer silicon beads coated with silicon nitride as seed layer. Journal of Crystal Growth, 2016, 441, 124-130.	1.5	13
197	Investigation of p-type emitter layer materials for heterojunction barium disilicide thin film solar cells. Japanese Journal of Applied Physics, 2017, 56, 05DB04.	1.5	13
198	Effects of evaporation vapor composition and post-annealing conditions on carrier density of undoped BaSi ₂ evaporated films. Japanese Journal of Applied Physics, 2020, 59, SFFA05.	1.5	13

#	Article	IF	CITATIONS
199	Atomic hydrogen passivation for photoresponsivity enhancement of boron-doped p-BaSi2 films and performance improvement of boron-doped p-BaSi2/n-Si heterojunction solar cells. Journal of Applied Physics, 2020, 127, .	2.5	13
200	Investigation on the origin of preferred a -axis orientation of BaSi 2 films deposited on Si(100) by thermal evaporation. Materials Science in Semiconductor Processing, 2017, 72, 93-98.	4.0	13
201	Improved conversion efficiency of p-type BaSi ₂ /n-type crystalline Si heterojunction solar cells by a low growth rate deposition of BaSi ₂ . AIP Advances, 2022, 12, 045115.	1.3	13
202	Optical Detection of Interdiffusion in StrainedSi1-xGex/SiQuantum Well Structures. Japanese Journal of Applied Physics, 1994, 33, 2344-2347.	1.5	12
203	Precise control of island formation using overgrowth technique on cleaved edges of strained multiple quantum wells. Applied Physics Letters, 1997, 70, 2981-2983.	3.3	12
204	Phase diagram calculation for epitaxial growth of GaInAs on InP considering the surface, interfacial and strain energies. Journal of Crystal Growth, 2000, 220, 413-424.	1.5	12
205	Molten metal flux growth and properties of CrSi2. Journal of Alloys and Compounds, 2004, 383, 319-321.	5.5	12
206	Modification of local structures in multicrystals revealed by spatially resolved x-ray rocking curve analysis. Journal of Applied Physics, 2007, 102, 103504.	2.5	12
207	Application of SiGe bulk crystal as a substrate for strain-controlled heterostructure materials. Thin Solid Films, 2008, 517, 14-16.	1.8	12
208	Towards implementation of floating cast method for growing large-scale high-quality multicrystalline silicon ingot using designed double crucibles. Progress in Photovoltaics: Research and Applications, 2014, 22, 726-732.	8.1	12
209	Relationship between dislocation density and contact angle of dendrite crystals in practical size silicon ingot. Journal of Applied Physics, 2015, 117, .	2.5	12
210	Development of spin-coated copper iodide on silicon for use in hole-selective contacts. Energy Procedia, 2017, 124, 598-603.	1.8	12
211	Evidence of solute PEDOT:PSS as an efficient passivation material for fabrication of hybrid c-Si solar cells. Sustainable Energy and Fuels, 2019, 3, 1448-1454.	4.9	12
212	Activation energy of hydrogen desorption from high-performance titanium oxide carrier-selective contacts with silicon oxide interlayers. Current Applied Physics, 2021, 21, 36-42.	2.4	12
213	Fabrication of heterojunction crystalline Si solar cells with BaSi ₂ thin films prepared by a two-step evaporation method. Japanese Journal of Applied Physics, 2021, 60, 105503.	1.5	12
214	Growth of SixGe1-x(\$x allingdotseq 0.15\$) Bulk Crystal with Uniform Composition Utilizingin situMonitoring of the Crystal-solution Interface. Japanese Journal of Applied Physics, 2001, 40, 4141-4144.	1.5	11
215	Impact of Defect Density in Si Bulk Multicrystals on Gettering Effect of Impurities. Japanese Journal of Applied Physics, 2008, 47, 8790-8792.	1.5	11
216	Direct bandgap measurements in a three-dimensionally macroporous silicon 9R polytype using monochromated transmission electron microscope. Applied Physics Letters, 2010, 97, .	3.3	11

#	Article	IF	CITATIONS
217	Ion dose, energy, and species dependencies of strain relaxation of SiGe buffer layers fabricated by ion implantation technique. Journal of Applied Physics, 2010, 107, 103509.	2.5	11
218	Structural Study of BF ₂ lon Implantation and Post Annealing of BaSi ₂ Epitaxial Films. Japanese Journal of Applied Physics, 2011, 50, 121202.	1.5	11
219	Formation of black silicon using SiGe self-assembled islands as a mask for selective anisotropic etching of silicon. Materials Science in Semiconductor Processing, 2018, 75, 143-148.	4.0	11
220	Influence of the time-dependent vapor composition on structural properties of the BaSi ₂ thin films fabricated by vacuum evaporation. Japanese Journal of Applied Physics, 2020, 59, SFFA10.	1.5	11
221	Silicon Nanocrystals Embedded in Nanolayered Silicon Oxide for Crystalline Silicon Solar Cells. ACS Applied Nano Materials, 2022, 5, 1820-1827.	5.0	11
222	Photogeneration and Transport of Carriers in Strained Si1-xGex/Si Quantum Well Structures. Japanese Journal of Applied Physics, 1992, 31, L1525-L1528.	1.5	10
223	Band-Edge Luminescence of Strained SixGe1-x/Si Single Quantum Well Structures Grown on Si(111) by Si Molecular Beam Epitaxy. Japanese Journal of Applied Physics, 1992, 31, L1018-L1020.	1.5	10
224	Cathodoluminescence investigation of SiGe quantum wires fabricated on V-groove patterned Si substrates. Journal of Crystal Growth, 1995, 150, 1070-1073.	1.5	10
225	Control of Macroscopic Absorption Coefficient of Multicrystalline SiGe by Microscopic Compositional Distribution. Japanese Journal of Applied Physics, 2002, 41, L37-L39.	1.5	10
226	Fabrication of SiGe-on-insulator by rapid thermal annealing of Ge on Si-on-insulator substrate. Applied Surface Science, 2004, 224, 95-98.	6.1	10
227	Thickness Dependence of Strain Field Distribution in SiGe Relaxed Buffer Layers. Japanese Journal of Applied Physics, 2005, 44, 8445-8447.	1.5	10
228	Growth temperature dependence of the crystalline morphology of SiGe films grown on Si(110) substrates with compositionally step-graded buffer. Thin Solid Films, 2008, 517, 235-238.	1.8	10
229	Strain relaxation mechanisms in compositionally uniform and step-graded SiGe films grown on Si(1 1) Tj ETQq1 1	0,784314 1.4	rgBT /Overlo
230	Room-Temperature Electroluminescence from Ge Quantum Dots Embedded in Photonic Crystal Microcavities. Applied Physics Express, 2012, 5, 052101.	2.4	10
231	Growth velocity and grain size of multicrystalline solar cell silicon. Journal of Crystal Growth, 2012, 356, 17-21.	1.5	10
232	Grazing-incidence small-angle X-ray scattering from Ge nanodots self-organized on Si(001) examinedÂwith soft X-rays. Journal of Synchrotron Radiation, 2014, 21, 161-164.	2.4	10
233	Carrier extraction dynamics from Ge/Si quantum wells in Si solar cells. Thin Solid Films, 2014, 557, 368-371.	1.8	10
234	Influence of Substrate on Crystal Orientation of Large-Grained Si Thin Films Formed by Metal-Induced Crystallization. International Journal of Photoenergy, 2015, 2015, 1-7.	2.5	10

#	Article	IF	CITATIONS
235	Effects of grain boundary structure controlled by artificially designed seeds on dislocation generation. Japanese Journal of Applied Physics, 2017, 56, 075501.	1.5	10
236	Improving the photoresponse spectra of BaSi2 layers by capping with hydrogenated amorphous Si layers prepared by radio-frequency hydrogen plasma. AIP Advances, 2018, 8, 055306.	1.3	10
237	Fine line Al printing on narrow point contact opening for front side metallization. AIP Conference Proceedings, 2019, , .	0.4	10
238	Undoped p-type BaSi ₂ emitter prepared by thermal evaporation and post-annealing for crystalline silicon heterojunction solar cells. Applied Physics Express, 2020, 13, 051002.	2.4	10
239	Zn _{1–<i>x</i>} Ge _{<i>x</i>} O _{<i>y</i>} Passivating Interlayers for BaSi ₂ Thin-Film Solar Cells. ACS Applied Materials & Interfaces, 2022, 14, 13828-13835.	8.0	10
240	Data-Driven Optimization and Experimental Validation for the Lab-Scale Mono-Like Silicon Ingot Growth by Directional Solidification. ACS Omega, 2022, 7, 6665-6673.	3.5	10
241	Self-modulating Sb incorporation in Si/SiGe superlattices during molecular beam epitaxial growth. Surface Science, 1993, 295, 335-339.	1.9	9
242	Evidence of the Presence of Built-in Strain in Multicrystalline SiGe with Large Compositional Distribution. Japanese Journal of Applied Physics, 2002, 41, 4462-4465.	1.5	9
243	Low-temperature growth of single-crystalline ZnO tubes on sapphire(0001) substrates. Applied Physics A: Materials Science and Processing, 2004, 79, 1711-1714.	2.3	9
244	Effects of vicinal steps on the island growth and orientation of epitaxially grown perylene-3,4,9,10-tetracarboxylic dianhydride (PTCDA) thin film crystals on a hydrogen-terminated Si(111) substrate. Journal of Crystal Growth, 2005, 273, 594-602.	1.5	9
245	Changes in elastic deformation of strained Si by microfabrication. Materials Science in Semiconductor Processing, 2005, 8, 181-185.	4.0	9
246	Observation of strain field fluctuation in SiGe-relaxed buffer layers and its influence on overgrown structures. Materials Science in Semiconductor Processing, 2005, 8, 177-180.	4.0	9
247	Floating Zone Growth of Si Bicrystals Using Seed Crystals with Artificially Designed Grain Boundary Configuration. Japanese Journal of Applied Physics, 2005, 44, L778-L780.	1.5	9
248	Fabrication of thin strain-relaxed SiGe buffer layers with high Ge composition by ion implantation method. Journal of Crystal Growth, 2009, 311, 825-828.	1.5	9
249	Line Width Dependence of Anisotropic Strain State in SiGe Films Induced by Selective Ion Implantation. Applied Physics Express, 2011, 4, 095701.	2.4	9
250	Formation of compressively strained Si/Si1â^'xCx/Si(100) heterostructures using gas-source molecular beam epitaxy. Journal of Crystal Growth, 2013, 362, 276-281.	1.5	9
251	On the growth mechanism of polycrystalline silicon thin film by Al-induced layer exchange process. Journal of Crystal Growth, 2013, 362, 16-19.	1.5	9
252	Enhanced photocarrier generation in large-scale photonic nanostructures fabricated from vertically aligned quantum dots. Optics Express, 2014, 22, A225.	3.4	9

#	Article	IF	CITATIONS
253	Control of geometry in Si-based photonic nanostructures formed by maskless wet etching process and its impact on optical properties. Thin Solid Films, 2014, 557, 338-341.	1.8	9
254	Effect of passivation layer grown by atomic layer deposition and sputtering processes on Si quantum dot superlattice to generate high photocurrent for high-efficiency solar cells. Japanese Journal of Applied Physics, 2016, 55, 032303.	1.5	9
255	Controlling impurity distributions in crystalline Si for solar cells by using artificial designed defects. Journal of Crystal Growth, 2017, 468, 610-613.	1.5	9
256	Boron-doped p-BaSi2/n-Si solar cells formed on textured n-Si(0 0 1) with a pyramid structure consisting of {1 1 1} facets. Journal of Crystal Growth, 2017, 475, 186-191.	1.5	9
257	Selective etching of Si, SiGe, Ge and its usage for increasing the efficiency of silicon solar cells. Semiconductors, 2017, 51, 1542-1546.	0.5	9
258	Fabrication of BaSi2 thin films capped with amorphous Si using a single evaporation source. Thin Solid Films, 2017, 636, 546-551.	1.8	9
259	Post-annealing effects on the surface structure and carrier lifetime of evaporated BaSi ₂ films. Japanese Journal of Applied Physics, 2017, 56, 04CS07.	1.5	9
260	Impact of size distributions of Ge islands as etching masks for anisotropic etching on formation of anti-reflection structures. Japanese Journal of Applied Physics, 2019, 58, 045505.	1.5	9
261	Effect of Phase Purity on Dislocation Density of Pressurized-Reactor Metalorganic Vapor Phase Epitaxy Grown InN. Japanese Journal of Applied Physics, 2012, 51, 04DH02.	1.5	9
262	Band-edge photoluminescence of SiGe/strained-Si/SiGe type-II quantum wells on Si(100). Solid-State Electronics, 1994, 37, 933-936.	1.4	8
263	Field-driven blue shift of excitonic photoluminescence in Siî—,Ge quantum wells and superlattices. Journal of Crystal Growth, 1995, 157, 40-44.	1.5	8
264	Improved luminescence quality with an asymmetric confinement potential in Si-based type-II quantum wells grown on a graded SiGe relaxed buffer. Journal of Vacuum Science & Technology an Official Journal of the American Vacuum Society B, Microelectronics Processing and Phenomena, 1996, 14, 2387.	1.6	8
265	Drastic increase of the density of Ge islands by capping with a thin Si layer. Applied Physics Letters, 2000, 77, 217-219.	3.3	8
266	Fabrication of SiGe-on-Insulator through Thermal Diffusion of Ge on Si-on-Insulator Substrate. Japanese Journal of Applied Physics, 2003, 42, L232-L234.	1.5	8
267	Structural and Optical Properties of ZnO Epitaxial Films Grown on Al2O3(11ar20) Substrates by Metalorganic Chemical Vapor Deposition. Japanese Journal of Applied Physics, 2004, 43, 4110-4113.	1.5	8
268	Growth and properties of SiGe multicrystals with microscopic compositional distribution and their applications for high-efficiency solar cells. Journal of Crystal Growth, 2005, 275, e455-e460.	1.5	8
269	SiGe double barrier resonant tunneling diodes on bulk SiGe substrates with high peak-to-valley current ratio. Applied Physics Letters, 2007, 91, .	3.3	8
270	Growth behavior of faceted Si crystals at grain boundary formation. Journal of Crystal Growth, 2009, 312, 19-23.	1.5	8

#	Article	IF	CITATIONS
271	Epitaxial Growth and Photoresponse Properties of BaSi2Layers toward Si-Based High-Efficiency Solar Cells. Japanese Journal of Applied Physics, 2010, 49, 04DP05.	1.5	8
272	Large-Grain Polycrystalline Silicon Films Formed through Flash-Lamp-Induced Explosive Crystallization. Japanese Journal of Applied Physics, 2012, 51, 10NB15.	1.5	8
273	Potential variation around grain boundaries in BaSi2 films grown on multicrystalline silicon evaluated using Kelvin probe force microscopy. Journal of Applied Physics, 2014, 116, .	2.5	8
274	Enhanced Phosphorus Gettering of Impurities in Multicrystalline Silicon at Low Temperature. Energy Procedia, 2014, 55, 203-210.	1.8	8
275	Hole mobility in strained Si/SiGe/vicinal Si(110) grown by gas source MBE. Journal of Crystal Growth, 2017, 468, 625-629.	1.5	8
276	Controlling impurity distribution in quasi-mono crystalline Si ingot by seed manipulation for artificially controlled defects technique. Energy Procedia, 2017, 124, 734-739.	1.8	8
277	Determination of carrier recombination velocity at inclined grain boundaries in multicrystalline silicon through photoluminescence imaging and carrier simulation. Journal of Applied Physics, 2020, 128, 125103.	2.5	8
278	Significant enhancement of photoresponsivity in As-doped n-BaSi ₂ epitaxial films by atomic hydrogen passivation. Applied Physics Express, 2020, 13, 051001.	2.4	8
279	Mechanisms of carrier lifetime enhancement and conductivity-type switching on hydrogen-incorporated arsenic-doped BaSi2. Thin Solid Films, 2021, 724, 138629.	1.8	8
280	Generation of dislocation clusters at triple junctions of random angle grain boundaries during cast growth of silicon ingots. Applied Physics Express, 2020, 13, 105505.	2.4	8
281	Strain-induced lateral band gap modulation in Si1â^'xGex/Si quantum well and quantum wire structures. Journal of Crystal Growth, 1995, 150, 1065-1069.	1.5	7
282	Electrical properties of N2O/NH3 plasma grown oxynitride on strained-Si. IEEE Electron Device Letters, 1998, 19, 273-275.	3.9	7
283	Molecular beam epitaxy of GaAs on nearly lattice-matched SiGe substrates grown by the multicomponent zone-melting method. Semiconductor Science and Technology, 2001, 16, 699-703.	2.0	7
284	Fabrication of strain-balanced Si/Si1â^'xGex multiple quantum wells on Si1â^'yGey virtual substrates and their optical properties. Applied Physics Letters, 2001, 79, 344-346.	3.3	7
285	Preparation of a TiO ₂ Film Coated Si Device for Photo-Decomposition of Water by CVD Method Using Ti(OPr ⁱ) ₄ . Materials Transactions, 2002, 43, 1533-1536.	1.2	7
286	Simultaneous in situ measurement of solute and temperature distributions in the alloy solutions. Journal of Crystal Growth, 2002, 242, 313-320.	1.5	7
287	Planarization of SiGe virtual substrates by CMP and its application to strained Si modulation-doped structures. Journal of Crystal Growth, 2003, 251, 693-696.	1.5	7
288	Fabrication of solar cell with stacked Ge islands for enhanced absorption in the infrared regime. Thin Solid Films, 2004, 451-452, 604-607.	1.8	7

#	Article	IF	CITATIONS
289	Low-temperature growth of ZnO epitaxial films by metal organic chemical vapor deposition. Applied Physics A: Materials Science and Processing, 2004, 78, 25-28.	2.3	7
290	Effects of growth temperature on the surface morphology of silicon thin films on (111) silicon monocrystalline substrate by liquid phase epitaxy. Journal of Crystal Growth, 2004, 266, 467-474.	1.5	7
291	Improvement in the conversion efficiency of single-junction SiGe solar cells by intentional introduction of the compositional distribution. Journal of Applied Physics, 2007, 101, 054504.	2.5	7
292	Development of Thin SiGe Relaxed Layers with High-Ge Composition by Ion Implantation Method and Application to Strained Ge Channels. Applied Physics Express, 0, 1, 081401.	2.4	7
293	Resonant photoluminescence from Ge self-assembled dots in optical microcavities. Journal of Crystal Growth, 2009, 311, 883-887.	1.5	7
294	Impact of amorphous Ge thin layer at the amorphous Si/Al interface on Al-induced crystallization. Journal of Crystal Growth, 2010, 312, 3257-3260.	1.5	7
295	A grazing incidence small-angle x-ray scattering analysis on capped Ge nanodots in layer structures. Journal of Physics Condensed Matter, 2010, 22, 474003.	1.8	7
296	Generation of high photocurrent in three-dimensional silicon quantum dot superlattice fabricated by combining bio-template and neutral beam etching for quantum dot solar cells. Nanoscale Research Letters, 2013, 8, 228.	5.7	7
297	Effect of Ga content and growth temperature on Cu(In,Ga)Se ₂ thin film deposited on heatâ€resistant glass substrates. Physica Status Solidi C: Current Topics in Solid State Physics, 2013, 10, 1035-1037.	0.8	7
298	Control of Dip Shape in Photonic Nanostructures by Maskless Wet-Etching Process and Its Impact on Optical Properties. Japanese Journal of Applied Physics, 2013, 52, 080202.	1.5	7
299	Al-induced crystallization of amorphous Ge thin films on conducting layer coated glass substrates. Japanese Journal of Applied Physics, 2014, 53, 04EH01.	1.5	7
300	Structural characterization of polycrystalline Ge thin films on insulators formed by diffusion-enhanced Al-induced layer exchange. Japanese Journal of Applied Physics, 2014, 53, 04EH03.	1.5	7
301	Large-grained (111)-oriented Si/Al/SiO2 structures formed by diffusion-controlled Al-induced layer exchange. Thin Solid Films, 2014, 557, 147-150.	1.8	7
302	Growth of strained Si/relaxed SiGe heterostructures on Si(110) substrates using solid-source molecular beam epitaxy. Semiconductor Science and Technology, 2017, 32, 114002.	2.0	7
303	Minority-carrier lifetime and photoresponse properties of B-doped p-BaSi ₂ , a potential light absorber for solar cells. Japanese Journal of Applied Physics, 2017, 56, 05DB01.	1.5	7
304	Effect of substrate type on the electrical and structural properties of TiO2 thin films deposited by reactive DC sputtering. Journal of Crystal Growth, 2018, 491, 120-125.	1.5	7
305	Fabrication of light-trapping structure by selective etching of thin Si substrates masked with a Ge dot layer and nanomasks. Japanese Journal of Applied Physics, 2018, 57, 08RF09.	1.5	7
306	Fabrication of Si1-xGex layer on Si substrate by Screen-Printing. MRS Advances, 2019, 4, 749-754.	0.9	7

#	Article	IF	CITATIONS
307	The impact of highly excessive PbI ₂ on the correlation of MAPbI ₃ perovskite morphology and carrier lifetimes. Journal of Materials Chemistry C, 2020, 8, 14481-14489.	5.5	7
308	Impact of deposition of indium tin oxide double layers on hydrogenated amorphous silicon/crystalline silicon heterojunction. AIP Advances, 2020, 10, 065008.	1.3	7
309	Point defects in BaSi2 thin films for photovoltaic applications studied by positron annihilation spectroscopy. Journal of Applied Physics, 2020, 127, .	2.5	7
310	Fabrication of Silicon Nanowire Metal-Oxide-Semiconductor Capacitors with Al2O3/TiO2/Al2O3 Stacked Dielectric Films for the Application to Energy Storage Devices. Energies, 2021, 14, 4538.	3.1	7
311	Application of Bayesian optimization for high-performance TiO /SiO /c-Si passivating contact. Solar Energy Materials and Solar Cells, 2021, 230, 111251.	6.2	7
312	Origin of recombination activity of non-coherent Σ3{111} grain boundaries with a positive deviation in the tilt angle in cast-grown silicon ingots. Applied Physics Express, 2021, 14, 011002.	2.4	7
313	Observation of electroluminescence above room temperature in strained p-type Si0.65Ge0.35/Si(111) multiple quantum wells. Journal of Crystal Growth, 1993, 127, 1083-1087.	1.5	6
314	Band-Edge Photoluminescence of SiGe/Strained-Si/SiGe Type-II Quantum Wells on Si(100). Japanese Journal of Applied Physics, 1993, 32, L1391-L1393.	1.5	6
315	Intense photoluminescence from Si-based quantum well structures with neighboring confinement structure. Journal of Crystal Growth, 1995, 157, 27-30.	1.5	6
316	Dynamics of exciton diffusion in SiGe quantum wells on assV-groove patterned Si substrate. Physical Review B, 1995, 52, 5132-5135.	3.2	6
317	Spectroscopic study of Si-based quantum wells with neighbouring confinement structure. Semiconductor Science and Technology, 1997, 12, 1596-1602.	2.0	6
318	Magneto-photoluminescence spectra of GaP/AlP short-period superlattices in high magnetic fields and uniaxial pressures. Physica B: Condensed Matter, 1998, 249-251, 909-913.	2.7	6
319	Wavy interface morphologies in strained multilayers on vicinal Si(111) substrates. Journal of Physics Condensed Matter, 1998, 10, 8643-8652.	1.8	6
320	In SituMeasurement of Composition in High-Temperature Solutions by X-Ray Fluorescence Spectrometry. Japanese Journal of Applied Physics, 2000, 39, 5981-5982.	1.5	6
321	In situ observation of the Marangoni convection in a NaCl aqueous solutions under microgravity. Journal of Crystal Growth, 2002, 234, 516-522.	1.5	6
322	3D atomic imaging of SiGe system by X-ray fluorescence holography. Journal of Materials Science: Materials in Electronics, 2003, 14, 459-462.	2.2	6
323	High-Quality Crystalline Silicon Layer Grown by Liquid Phase Epitaxy Method at Low Growth Temperature. Japanese Journal of Applied Physics, 2003, 42, L217-L219.	1.5	6
324	Liquid Phase Epitaxial Growth of Si Layers on Si Thin Substrates from Si Pure Melts under Near-Equilibrium Conditions. Japanese Journal of Applied Physics, 2005, 44, 5092-5095.	1.5	6

#	Article	IF	CITATIONS
325	Application of Czochralski-grown SiGe bulk crystal as a substrate for luminescent strained quantum wells. Applied Physics Letters, 2007, 90, 181914.	3.3	6
326	Effects of increased compressive strain on hole effective mass and scattering mechanisms in strained Ge channels. Microelectronic Engineering, 2011, 88, 465-468.	2.4	6
327	Influence of Thermal Annealing on the Carrier Extraction in Ge/Si Quantum Dot Solar Cells. Japanese Journal of Applied Physics, 2012, 51, 10NE24.	1.5	6
328	Light trapping by direction-dependent light transmission in front-surface photonic nanostructures. Applied Physics Express, 2014, 7, 122301.	2.4	6
329	Suppression of metastable-phase inclusion in N-polar (0001Â ⁻) InGaN/GaN multiple quantum wells grown by metalorganic vapor phase epitaxy. Applied Physics Letters, 2015, 106, .	3.3	6
330	Effect of grain boundary character of multicrystalline Si on external and internal (phosphorus) gettering of impurities. Progress in Photovoltaics: Research and Applications, 2016, 24, 1615-1625.	8.1	6
331	Control of electrical properties of BaSi2 thin films by alkali-metal doping using alkali-metal fluorides. Thin Solid Films, 2016, 603, 218-223.	1.8	6
332	Towards optimized nucleation control in multicrystalline silicon ingot for solar cells. Journal of Crystal Growth, 2017, 468, 620-624.	1.5	6
333	Suppression of Near-interface Oxidation in Thermally-evaporated BaSi2 Films and Its Effects on Preferred Orientation and the Rectification Behavior of n-BaSi2/p+-Si Diodes. MRS Advances, 2018, 3, 1387-1392.	0.9	6
334	Tuning the Electrical Properties of Titanium Oxide Bilayers Prepared by Atomic Layer Deposition at Different Temperatures. Physica Status Solidi (A) Applications and Materials Science, 2019, 216, 1900495.	1.8	6
335	Drastic enhancement of photoresponsivity in C-doped BaSi2 films formed by radio-frequency sputtering. Japanese Journal of Applied Physics, 2020, 59, SFFA06.	1.5	6
336	Passivation mechanism of the high-performance titanium oxide carrier-selective contacts on crystalline silicon studied by spectroscopic ellipsometry. Japanese Journal of Applied Physics, 2021, 60, SBBF04.	1.5	6
337	Impact of chemically grown silicon oxide interlayers on the hydrogen distribution at hydrogenated amorphous silicon/crystalline silicon heterointerfaces. Applied Surface Science, 2021, 567, 150799.	6.1	6
338	Effect of the Niobium-Doped Titanium Oxide Thickness and Thermal Oxide Layer for Silicon Quantum Dot Solar Cells as a Dopant-Blocking Layer. Nanoscale Research Letters, 2020, 15, 39.	5.7	6
339	Photoluminescence of Si/SiGe/Si quantum wells on separation by oxygen implantation substrate. Applied Physics Letters, 1994, 64, 2373-2375.	3.3	5
340	Rectangular AlGaAs/AlAs Quantum Wires Using Spontaneous Vertical Quantum Wells. Japanese Journal of Applied Physics, 1996, 35, 1214-1216.	1.5	5
341	Interfacial roughness of multilayer structures on Si(111) probed by x-ray scattering. Journal of Physics Condensed Matter, 1997, 9, 4521-4533.	1.8	5
342	Effects of tensile strain on the optical properties of an AlGaP-based neighbouring confinement structure. Semiconductor Science and Technology, 1997, 12, 881-887.	2.0	5

#	Article	IF	CITATIONS
343	Effect of the insertion of an ultrathin AlP layer on the optical properties of GaAsP/GaP quantum wells. Physical Review B, 1999, 60, 13735-13739.	3.2	5
344	Fabrication of SiGe bulk crystals with uniform composition as substrates for Si-based heterostructures. Materials Science and Engineering B: Solid-State Materials for Advanced Technology, 2002, 89, 364-367.	3.5	5
345	Crystal Quality Evaluation of 6H-SiC Layers Grown by Liquid Phase Epitaxy around Micropipes using Micro-Raman Scattering Spectroscopy. Materials Science Forum, 2004, 457-460, 633-636.	0.3	5
346	Growth of InGaAs and SiGe homogeneous bulk crystals which have complete miscibility in the phase diagrams. International Journal of Materials and Product Technology, 2005, 22, 185.	0.2	5
347	Strain-Field Evaluation of Strain-Relaxed Thin SiGe Layers Fabricated by Ion Implantation Method. Japanese Journal of Applied Physics, 2005, 44, L1316-L1319.	1.5	5
348	On the Origin of Improved Conversion Efficiency of Solar Cells Based on SiGe with Compositional Distribution. Japanese Journal of Applied Physics, 2005, 44, 857-860.	1.5	5
349	Strain field and related roughness formation in SiGe relaxed buffer layers. Thin Solid Films, 2006, 508, 117-119.	1.8	5
350	Poly-Si films with long carrier lifetime prepared by rapid thermal annealing of Cat-CVD amorphous silicon thin films. Thin Solid Films, 2008, 516, 600-603.	1.8	5
351	On Effects of Gate Bias on Hole Effective Mass and Mobility in Strained-Ge Channel Structures. Applied Physics Express, 2008, 1, 011401.	2.4	5
352	High efficiency solar cells obtained from small size ingots with 30 cmΦ by controlling the distribution and orientation of dendrite crystals grown along the bottom of the ingots. , 2010, , .		5
353	Effect of Phase Purity on Dislocation Density of Pressurized-Reactor Metalorganic Vapor Phase Epitaxy Grown InN. Japanese Journal of Applied Physics, 2012, 51, 04DH02.	1.5	5
354	Formation of large-grain-sized BaSi2 epitaxial layers grown on Si(111) by molecular beam epitaxy. Journal of Crystal Growth, 2013, 378, 193-197.	1.5	5
355	Control of surface dip diameter in Si-based photonic nanostructures by changing growth temperature of Ge quantum dot multilayer structures and its impact on their optical properties. Japanese Journal of Applied Physics, 2015, 54, 08KA01.	1.5	5
356	Cross-sectional potential profile across a BaSi2pn junction by Kelvin probe force microscopy. Japanese Journal of Applied Physics, 2015, 54, 030306.	1.5	5
357	Evidence for efficient passivation of vertical silicon nanowires by anodic aluminum oxide. Solar Energy Materials and Solar Cells, 2016, 157, 393-398.	6.2	5
358	On the growth mechanism of multicrystalline silicon ingots with small grains fabricated using single-layer silicon beads. Japanese Journal of Applied Physics, 2017, 56, 075502.	1.5	5
359	Growth of BaSi ₂ film on Ge(100) by vacuum evaporation and its photoresponse properties. Japanese Journal of Applied Physics, 2017, 56, 05DB06.	1.5	5
360	Fabrication of silicon nanowire based solar cells using TiO2/Al2O3 stack thin films. MRS Advances, 2018, 3, 1419-1426.	0.9	5

#	Article	IF	CITATIONS
361	Epitaxial growth of SiGe on Si substrate by printing and firing of Al–Ge mixed paste. Japanese Journal of Applied Physics, 2019, 58, 045504.	1.5	5
362	Impact of Ge deposition temperature on parameters of c-Si solar cells with surface texture formed by etching of Si using SiGe islands as a mask. Materials Science in Semiconductor Processing, 2020, 114, 105065.	4.0	5
363	Effect of forming gas annealing on hydrogen content and surface morphology of titanium oxide coated crystalline silicon heterocontacts. Journal of Vacuum Science and Technology A: Vacuum, Surfaces and Films, 2020, 38, 022415.	2.1	5
364	Propagation of Crystal Defects during Directional Solidification of Silicon via Induction of Functional Defects. Crystals, 2021, 11, 90.	2.2	5
365	<i>In situ</i> Observation of Polycrystalline Silicon Thin Films Grown Using Aluminum-Doped Zinc Oxide on Glass Substrate by the Aluminum-Induced Crystallization. Japanese Journal of Applied Physics, 2011, 50, 04DP02.	1.5	5
366	Characterization of SiGe quantum wire structures by cathodoluminescence imaging and spectroscopy. Applied Physics Letters, 1995, 67, 1709-1711.	3.3	4
367	Magnetophotoluminescence spectroscopy of AlGaP-based neighboring confinement structures. Physical Review B, 1999, 60, 1879-1883.	3.2	4
368	Gas source molecular beam epitaxy grown strained-Si films on step-graded relaxed Si1â^'xGex for MOS applications. Journal of Electronic Materials, 1999, 28, 98-104.	2.2	4
369	Observation of negatively charged excitons and excited states of multi-excitons in quantum dots embedded in modulation doping structures. Physica E: Low-Dimensional Systems and Nanostructures, 2001, 11, 68-71.	2.7	4
370	PHONON REPLICA OF FREE EXCITONS IN ZnO EPITAXIAL FILMS. Nonlinear Optics, Quantum Optics, 2002, 29, 621-627.	0.2	4
371	Evaluation of the diffusion coefficients in liquid GaGe binary alloys using a novel method based on Fick's first law. Journal of Non-Crystalline Solids, 2002, 312-314, 196-202.	3.1	4
372	Improvement in the luminescence efficiency of GaAsN alloys by photoexcitation. Physica Status Solidi C: Current Topics in Solid State Physics, 2003, 0, 2782-2784.	0.8	4
373	Suppression of structural imperfection in strained Si by utilizing SiGe bulk substrate. Applied Physics Letters, 2006, 88, 221912.	3.3	4
374	Room-temperature light-emission from Ge quantum dots in photonic crystals. Thin Solid Films, 2008, 517, 125-127.	1.8	4
375	Structural and transport properties of strained SiGe grown on V-groove patterned Si(110) substrates. Journal of Crystal Growth, 2009, 311, 814-818.	1.5	4
376	Optical anisotropies of Si grown on step-graded SiGe(110) layers. Applied Physics Letters, 2010, 96, 091904.	3.3	4
377	On the origin of the uniaxial strain induced in Si/Ge heterostructures with selective ion implantation technique. Journal of Crystal Growth, 2013, 378, 251-253.	1.5	4
378	Large photoresponsivity in semiconducting BaSi2 epitaxial films grown on Si(001) substrates by molecular beam epitaxy. Journal of Crystal Growth, 2013, 378, 198-200.	1.5	4

#	Article	IF	CITATIONS
379	Simple approach for improving gold deposition inside nanoporous alumina template on Si substrate. Applied Surface Science, 2014, 305, 9-15.	6.1	4
380	Modulated surface nanostructures for enhanced light trapping and reduced surface reflection of crystalline silicon solar cells. Japanese Journal of Applied Physics, 2016, 55, 052302.	1.5	4
381	Effect of ALD-Al2O3 Passivated Silicon Quantum Dot Superlattices on p/i/n+ Solar Cells. IEEE Transactions on Electron Devices, 2017, 64, 2886-2892.	3.0	4
382	Application of weighted Voronoi diagrams to analyze nucleation sites of multicrystalline silicon ingots. Journal of Crystal Growth, 2018, 499, 62-66.	1.5	4
383	Formation of light-trapping structure using Ge islands grown by gas-source molecular beam epitaxy as etching masks. Japanese Journal of Applied Physics, 2018, 57, 08RB04.	1.5	4
384	High-Quality Si Multicrystals with Same Grain Orientation and Large Grain Size by the Newly Developed Dendritic Casting Method for High-Efficiency Solar Cell Applications. Advances in Materials Research, 2008, , 123-140.	0.2	4
385	Large-Grain Polycrystalline Silicon Films Formed through Flash-Lamp-Induced Explosive Crystallization. Japanese Journal of Applied Physics, 2012, 51, 10NB15.	1.5	4
386	Effects of grain boundary structure and shape of the solid–liquid interface on the growth direction of the grain boundaries in multicrystalline silicon. CrystEngComm, 2022, 24, 1948-1954.	2.6	4
387	Intense photoluminescence from strained Si1-xGexâ§,Si quantum well structures. Journal of Crystal Growth, 1993, 127, 489-493.	1.5	3
388	Anomalous spectral shift of photoluminescence from MBE-grown strained quantum wells mediated by atomic hydrogen. Journal of Crystal Growth, 1995, 157, 36-39.	1.5	3
389	Anomalous photoluminescence of pure-Ge/Si type-II coupled quantum wells (II-CQWs). Thin Solid Films, 1997, 294, 336-339.	1.8	3
390	Luminescence study on Ge islands as stressors on quantum well. Journal of Crystal Growth, 1997, 175-176, 519-523.	1.5	3
391	New strain-relieving microstructure in pure-Ge/Si short-period superlattices. Journal of Vacuum Science & Technology an Official Journal of the American Vacuum Society B, Microelectronics Processing and Phenomena, 1998, 16, 1595.	1.6	3
392	Correlation between electronic states and optical properties in indirect GaAsP/GaP quantum wells with insertion of an ultrathin AlP layer. Physica E: Low-Dimensional Systems and Nanostructures, 2000, 8, 323-327.	2.7	3
393	High-Temperature Solution Growth and Characterization of Chromium Disilicide. Japanese Journal of Applied Physics, 2003, 42, 7292-7293.	1.5	3
394	Growth of SiGe-on-insulator and its application as a substrate for epitaxy of strained-Si layer. Journal of Crystal Growth, 2005, 275, e1203-e1207.	1.5	3
395	Influence of stacked Ge islands on the dark current–voltage characteristics and the conversion efficiency of the solar cells. Thin Solid Films, 2006, 508, 402-405.	1.8	3
396	Intermixing of Ge and Si during exposure of GeH4 on Si. Thin Solid Films, 2006, 508, 163-165.	1.8	3

#	Article	IF	CITATIONS
397	High-Efficiency Concave and Conventional Solar Cell Integration System Using Focused Reflected Light. Japanese Journal of Applied Physics, 2006, 45, 1664-1667.	1.5	3
398	Control of strain status in SiGe thin film by epitaxial growth on Si with buried porous layer. Applied Physics Letters, 2007, 90, 031915.	3.3	3
399	Influence of growth temperature and cooling rate on the growth of Si epitaxial layer by dropping-type liquid phase epitaxy from the pure Si melt. Journal of Crystal Growth, 2008, 310, 5248-5251.	1.5	3
400	Vacancy formation during oxidation of silicon crystal surface. Applied Physics Letters, 2008, 93, 101904.	3.3	3
401	Local control of strain in SiGe by ion-implantation technique. Journal of Crystal Growth, 2009, 311, 806-808.	1.5	3
402	Ion energy and dose dependence of strain relaxation for thin SiGe buffer layers using Si+ implantation. Thin Solid Films, 2010, 518, S162-S164.	1.8	3
403	xmins:xocs= http://www.eisevier.com/xmi/xocs/dtd_xmins:xs= http://www.w3.org/2001/XMLSchema xmlns:xsi="http://www.w3.org/2001/XMLSchema-instance" xmlns="http://www.elsevier.com/xml/ja/dtd" xmlns:ja="http://www.elsevier.com/xml/ja/dtd" xmlns:mml="http://www.w3.org/1998/Math/MathML" xmlns:tb="http://www.elsevier.com/xml/common/table/dtd"	1.2	3
404	zmins:sb="http://www.elsevier.com/zmi/common/struct-bib/dtd" zmins:ce="http://www.elsevier.com/zmi/common/struct-bib/dtd" zmins:ce="http://www.elsevier.com/zmi/common 2011 Types of silicon–germanium (SiGe) bulk crystal growth methods and their applications. , 2011, , 72-82.		3
405	Selective growth of vertical silicon nanowire array guided by anodic aluminum oxide template. Japanese Journal of Applied Physics, 2015, 54, 095003.	1.5	3
406	Absorption enhancement in nanotextured solar cells with Ge/Si heterostructures. Japanese Journal of Applied Physics, 2015, 54, 04DR03.	1.5	3
407	Compressively strained Si/Si1â^xCxheterostructures formed on Ar ion implanted Si(100) substrates. Japanese Journal of Applied Physics, 2016, 55, 031302.	1.5	3
408	Novel light trapping structure by alkaline etching using a Ge dot mask for crystalline Si solar cells. , 2016, , .		3
409	Effects of surface morphology randomness on optical properties of Si-based photonic nanostructures. Japanese Journal of Applied Physics, 2017, 56, 08MA02.	1.5	3
410	Influence of barrier layer's height on the performance of Si quantum dot solar cells. Japanese Journal of Applied Physics, 2018, 57, 08RF08.	1.5	3
411	Impact of boron incorporation on properties of silicon solar cells employing p-type polycrystalline silicon grown by aluminum-induced crystallization. Japanese Journal of Applied Physics, 2018, 57, 08RB12.	1.5	3
412	Investigation of effective near-infrared light-trapping structure with submicron diameter for crystalline silicon thin film solar cells. Japanese Journal of Applied Physics, 2018, 57, 08RB21.	1.5	3
413	Improved Performance of Titanium Oxide/Silicon Oxide Electronâ€Selective Contacts by Implementation of Magnesium Interlayers. Physica Status Solidi (A) Applications and Materials Science, 2021, 218, 2100296.	1.8	3
414	(Invited) Engineering Strain, Defects, and Electronic Properties of (110)-Oriented Strained Si. ECS Transactions, 2020, 98, 277-290.	0.5	3

#	Article	IF	CITATIONS
415	Study on electrical activity of grain boundaries in silicon through systematic control of structural parameters and characterization using a pretrained machine learning model. Journal of Applied Physics, 2022, 132, .	2.5	3
416	Photoluminescence ofSi1-xGex/SiQuantum Wells with Abrupt Interfaces Formed by Segregant-Assisted Growth. Japanese Journal of Applied Physics, 1994, 33, 2304-2306.	1.5	2
417	Photoluminescence study of the optical properties of SiGe quantum wells on separation by implanted oxygen substrates. Journal of Applied Physics, 1997, 81, 3484-3489.	2.5	2
418	Enhanced no-phonon transition in indirect GaAsP/GaP quantum wells by insertion of monolayer AlP for electron localization. Journal of Crystal Growth, 1998, 188, 323-327.	1.5	2
419	In-plane potential modulation in tensilely strained AlGaP-based neighboring confinement structure. Physica E: Low-Dimensional Systems and Nanostructures, 1998, 2, 883-886.	2.7	2
420	Epitaxial growth and photoluminescence of Si/pure-Ge/Si quantum structures on Si(311) substrates. Semiconductor Science and Technology, 1998, 13, 1277-1283.	2.0	2
421	Strain distribution of Si thin film grown on multicrystalline-SiGe with microscopic compositional distribution. Journal of Applied Physics, 2002, 92, 7098-7101.	2.5	2
422	Relationship between Device Performance and Grain Boundary Structural Configuration in a Solar Cell Based on Multicrystalline SiGe. Japanese Journal of Applied Physics, 2004, 43, L250-L252.	1.5	2
423	Analysis of the Dark-Current Density in Solar Cells Based on Multicrystalline SiGe. Japanese Journal of Applied Physics, 2005, 44, 8019-8022.	1.5	2
424	Photo-induced improvement of radiative efficiency and structural changes in GaAsN alloys. Physica Status Solidi C: Current Topics in Solid State Physics, 2006, 3, 1907-1910.	0.8	2
425	Growth of Compositionally Graded SiGe Bulk Crystal and Its Application As Substrate with Lateral Variation in Ge Content. Japanese Journal of Applied Physics, 2009, 48, 115507.	1.5	2
426	Formation of uniaxially strained SiGe by selective ion implantation technique. Thin Solid Films, 2010, 518, 2454-2457.	1.8	2
427	Lattice-Latching Effect in Metalorganic Vapor Phase Epitaxy Growth of InGaAsN Film Lattice-Matched to Bulk InGaAs Substrate. Japanese Journal of Applied Physics, 2010, 49, 040202.	1.5	2
428	Fabrication of BaSi2 films on transparent CaF2 (111) substrates by molecular beam epitaxy for optical characterization. Physics Procedia, 2011, 11, 189-192.	1.2	2
429	Realization of Large-Domain Barium Disilicide Epitaxial Thin Film by Introduction of Miscut to Si(111) Substrate. Japanese Journal of Applied Physics, 2012, 51, 10NB06.	1.5	2
430	High photo-current generation in a three-dimensional silicon quantum dot superlattice fabricated by combination of bio-template and neutral beam etching for quantum dot solar cell. , 2013, , .		2
431	Gas-source MBE growth of strain-relaxed Si1â^'xCx on Si(100) substrates. Journal of Crystal Growth, 2013, 378, 212-217.	1.5	2
432	TEM Analysis of the Nanostructure of Pb(Mg _{1/3} Nb _{2/3})O ₃ Thin Films by MOD Method. Key Engineering Materials, 2013, 582, 19-22.	0.4	2

#	Article	IF	CITATIONS
433	Growth of vertical silicon nanowires array using electrochemical alternative. , 2013, , .		2
434	Nanostructure and Strain Field in Vertically Aligned Nano-Islands for Si/Ge 2D Photonic Nanocrystals Materials Research Society Symposia Proceedings, 2013, 1510, 1.	0.1	2
435	Effects of anodization process of aluminum oxide template fabrication on selective growth of Si nanowire arrays. Japanese Journal of Applied Physics, 2015, 54, 08KA02.	1.5	2
436	Growth direction control of dendrite crystals in parallel direction to realize high-quality multicrystalline silicon ingot. Japanese Journal of Applied Physics, 2016, 55, 091302.	1.5	2
437	Impact of anodic aluminum oxide fabrication and post-deposition anneal on the effective carrier lifetime of vertical silicon nanowires. Solar Energy Materials and Solar Cells, 2017, 166, 39-44.	6.2	2
438	Numerical simulation and performance optimization of perovskite solar cell. , 2017, , .		2
439	Fabrication and properties characterization of BaSi2 thin-films thermally-evaporated on Ge (100) modified substrates. Thin Solid Films, 2018, 663, 14-20.	1.8	2
440	Surface-orientation control of silicon thin films via aluminum-induced crystallization on monocrystalline cubic substrates. Journal of Crystal Growth, 2020, 533, 125441.	1.5	2
441	Scalable fabrication of GaN on amorphous substrates via MOCVD on highly oriented silicon seed layers. Journal of Crystal Growth, 2020, 535, 125522.	1.5	2
442	Simulation study on lateral minority carrier transport in the surface inversion layer of the p-aSi:H/i-aSi:H/cSi heterojunction solar cell. Japanese Journal of Applied Physics, 2021, 60, 026503.	1.5	2
443	Direct prediction of electrical properties of grain boundaries from photoluminescence profiles using machine learning. Applied Physics Letters, 2021, 119, .	3.3	2
444	Growth of High-Quality Polycrystalline Si Ingot with Same Grain Orientation by Using Dendritic Casting Method. Advances in Materials Research, 2008, , 141-147.	0.2	2
445	Fundamental Understanding of Subgrain Boundaries. Advances in Materials Research, 2009, , 83-95.	0.2	2
446	Epitaxy of Orthorhombic BaSi2with Preferential In-Plane Crystal Orientation on Si(001): Effects of Vicinal Substrate and Annealing Temperature. Japanese Journal of Applied Physics, 2012, 51, 095501.	1.5	2
447	Influence of Thermal Annealing on the Carrier Extraction in Ge/Si Quantum Dot Solar Cells. Japanese Journal of Applied Physics, 2012, 51, 10NE24.	1.5	2
448	Realization of crystalline BaSi2 thin films by vacuum evaporation on (111)-oriented Si layers fabricated by aluminum induced crystallization. , 0, , .		2
449	Preferred orientation of BaSi2 thin films fabricated by thermal evaporation. , 0, , .		2
450	Grazing-incidence Small-angle Scattering as a Tool for Thin Film Microstructure and Interface Analysis. Transactions of the Materials Research Society of Japan, 2007, 32, 275-280.	0.2	2

#	Article	IF	CITATIONS
451	Structural Study of BF2Ion Implantation and Post Annealing of BaSi2Epitaxial Films. Japanese Journal of Applied Physics, 2011, 50, 121202.	1.5	2
452	Molecular Beam Epitaxy of BaSi2Films with Grain Size over 4 µm on Si(111). Japanese Journal of Applied Physics, 2012, 51, 098003.	1.5	2
453	Fabrication of BaSi ₂ homojunction diodes on Nb-doped TiO ₂ coated glass substrates by aluminum-induced crystallization and two-step evaporation method. Japanese Journal of Applied Physics, 2022, 61, SC1029.	1.5	2
454	Estimation of Crystal Orientation of Grains on Polycrystalline Silicon Substrate by Recurrent Neural Network. IEEJ Transactions on Electrical and Electronic Engineering, 0, , .	1.4	2
455	A Si1â^'xGex/Si single quantum well p-i-n structure grown by solid-source and gas source "hybrid―Si molecular beam epitaxy. Journal of Crystal Growth, 1994, 136, 355-360.	1.5	1
456	Crucial role of Si buffer layer quality in the photoluminescence efficiency of strained Si1â ^{~,} xGex/Si quantum wells. Journal of Crystal Growth, 1995, 150, 1033-1037.	1.5	1
457	Timeâ€resolved photoluminescence study on AlxGa1â^'xAs spontaneous vertical quantum well structures. Applied Physics Letters, 1996, 68, 3221-3223.	3.3	1
458	Effect of tensile strain on optical properties of AlGaP-based neighboring confinement structure. Superlattices and Microstructures, 1998, 23, 97-102.	3.1	1
459	Control of island formation using overgrowth technique on cleaved edges of strained multiple quantum wells and selective epitaxy on patterned substrates. Physica E: Low-Dimensional Systems and Nanostructures, 1998, 2, 137-141.	2.7	1
460	Modification of the growth mode of Ge on Si(100) in the presence of buried Ge islands. Journal of Crystal Growth, 2001, 227-228, 782-785.	1.5	1
461	Successful Growth of InxGa1-xAs (x>0.18) Single Bulk Crystal Directly on GaAs Seed Crystal with Preferential Orientation. Japanese Journal of Applied Physics, 2004, 43, L907-L909.	1.5	1
462	Influence of growth temperature on minority-carrier lifetime of Si layer grown by liquid phase epitaxy using Ga solvent. Journal of Applied Physics, 2005, 98, 073708.	2.5	1
463	Development of Textured High-Quality Si Multicrystal Ingots with Same Grain Orientation and Large Grain Sizes by the New Dendritic Casting Method. , 2006, , .		1
464	High Sensitive Imaging of Atomic Arrangement of Ge Clusters Buried in a Si Crystal by X-ray Fluorescence Holography. Japanese Journal of Applied Physics, 2006, 45, 5248-5253.	1.5	1
465	Unique Temperature Dependence on the Morphological Evolution of Ge on Si(100). ECS Transactions, 2006, 3, 243-244.	0.5	1
466	Development of Textured High-Quality Si and SiGe Multicrystal Ingots with Same Grain Orientation and Large Grain Sizes by the New Dendritic Casting Method. ECS Transactions, 2006, 3, 265-267.	0.5	1
467	Fabrication of Ge channels with extremely high compressive strain and their magnetotransport properties. Journal of Crystal Growth, 2007, 301-302, 339-342.	1.5	1
468	Floating Cast Method as a New Growth Method of Silicon Bulk Multicrystals for Solar Cells. Advances in Materials Research, 2008, , 149-156.	0.2	1

#	Article	IF	CITATIONS
469	Evaluation of minority carrier lifetime in BaSi <inf>2</inf> as a novel material for earth-abundant high efficiency thin film solar cells. , 2010, , .		1
470	In situObservation of Polycrystalline Silicon Thin Films Grown Using Aluminum-Doped Zinc Oxide on Glass Substrate by the Aluminum-Induced Crystallization. Japanese Journal of Applied Physics, 2011, 50, 04DP02.	1.5	1
471	Growth of multicrystalline silicon ingot from the top of the melt: Control of microstructures and reduction of stress. , 2012, , .		1
472	Effect of Solid-Phase-Epitaxy Si Layers on Suppression of Sb Diffusion from Sb-Doped n ⁺ -BaSi ₂ /p ⁺ -Si Tunnel Junction to Undoped BaSi ₂ Overlayers. Japanese Journal of Applied Physics, 2012, 51, 04DP01.	1.5	1
473	Growth of multicrystalline Si ingots for solar cells using noncontact crucible method without touching the crucible wall. , 2012, , .		1
474	Lateral PIN current-injected photonic crystal nanocavity light emitting diodes based on Ge quantum dots. , 2012, , .		1
475	Type-II Ge/Si quantum dot superlattice for intermediate-band solar cell applications. , 2013, , .		1
476	Reflectance anisotropies of compressively strained Si grown on vicinal Si1â´'xCx(001). Applied Physics Letters, 2013, 102, 011902.	3.3	1
477	Nano-Structure around 90° Domain Wall and Elastic Interaction with Misfit Dislocation in PbTiO ₃ Thin Film. Key Engineering Materials, 2013, 566, 167-170.	0.4	1
478	Investigation of the tunneling properties and surface morphologies of BaSi2 /Si tunnel junctions for BaSi2 solar cell applications. Physica Status Solidi C: Current Topics in Solid State Physics, 2013, 10, 1765-1768.	0.8	1
479	Fabrication of BaSi2 films on (111)-oriented Si layers formed by inverted Al-induced crystallization method on glass structure. Physica Status Solidi C: Current Topics in Solid State Physics, 2013, 10, 1769-1772.	0.8	1
480	Epitaxial growth of BaSi2films with large grains using vicinal Si(111) substrates. Physica Status Solidi C: Current Topics in Solid State Physics, 2013, 10, 1756-1758.	0.8	1
481	Cross-sectional electric field distributions in BaSi2 homo and BaSi2/Si hetero pn junctions. , 2015, , .		1
482	Application of heterojunction to Si-based solar cells using photonic nanostructures coupled with vertically aligned Ge quantum dots. Japanese Journal of Applied Physics, 2015, 54, 08KA06.	1.5	1
483	Comparison of phosphorus gettering effect in faceted dendrite and small grain of multicrystalline silicon wafers grown by floating cast method. Japanese Journal of Applied Physics, 2015, 54, 08KD11.	1.5	1
484	Fabrication and characterization of BaSi2 films on Ge(111) substrates by molecular beam epitaxy. , 2015, , .		1
485	Application of new doping techniques to solar cells for low temperature fabrication. , 2016, , .		1
486	Light-induced Recovery of Effective Carrier Lifetime in Boron-doped Czochralski Silicon at Room Temperature. Energy Procedia, 2016, 92, 801-807.	1.8	1

#	Article	IF	CITATIONS
487	Optical characterization of double-side-textured silicon wafer based on photonic nanostructures for thin-wafer crystalline silicon solar cells. Japanese Journal of Applied Physics, 2017, 56, 04CS01.	1.5	1
488	Deposition and Characterization of Si Quantum Dot Multilayers Prepared by Plasma Enhanced Chemical Vapor Deposition using SiH <inf>4</inf> and CO <inf>2</inf> Gases. , 2018, , .		1
489	Evaluation of Si Nanowire MOS Capacitor Using High-k Dielectric Materials. , 2018, , .		1
490	Controllable Optical and Electrical Properties of Nb Doped TiO <inf>2</inf> Films by RF Sputtering. , 2018, , .		1
491	Mössbauer spectroscopic microscope study on diffusion and segregation of Fe impurities in mc-Si wafer. Hyperfine Interactions, 2019, 240, 1.	0.5	1
492	Pole figure analysis from electron backscatter diffraction—an effective method of evaluating fiber-textured silicon thin films as seed layers for epitaxy. Applied Physics Express, 2019, 12, 025501.	2.4	1
493	Effects of Surface Doping of Si Absorbers on the Band Alignment and Electrical Performance of TiO2-Based Electron-Selective Contacts. MRS Advances, 2019, 4, 769-775.	0.9	1
494	Synthesis of Mg ₂ Si thin film by thermal treatment under inert gas atmosphere and evaluation of film quality. Japanese Journal of Applied Physics, 2020, 59, SFFB03.	1.5	1
495	Preparation and thermoelectric characterization of phosphorus-doped Si nanocrystals/silicon oxide multilayers. Japanese Journal of Applied Physics, 2020, 59, SGGF09.	1.5	1
496	Effect of Si substrate modification on improving the crystalline quality, optical and electrical properties of thermally-evaporated BaSi2 thin-films for solar cell applications. International Journal of Modern Physics B, 2020, 34, 2050068.	2.0	1
497	Occurrence Prediction of Dislocation Regions in Photoluminescence Image of Multicrystalline Silicon Wafers Using Transfer Learning of Convolutional Neural Network. IEICE Transactions on Fundamentals of Electronics, Communications and Computer Sciences, 2021, E104.A, 857-865.	0.3	1
498	Contact control of Al/Si interface of Si solar cells by local contact opening method. Materials Chemistry and Physics, 2021, 270, 124833.	4.0	1
499	Formation and Properties of SiGe/Si Quantum Wire Structures. , 1995, , 151-160.		1
500	Surface inversion layer effective minority carrier mobility as one of the measures of surface quality of the p-aSi:H/i-aSi:H/cSi heterojunction solar cell. Japanese Journal of Applied Physics, 2020, 59, SGGF06.	1.5	1
501	Effect of Solid-Phase-Epitaxy Si Layers on Suppression of Sb Diffusion from Sb-Doped n ⁺ -BaSi ₂ /p ⁺ -Si Tunnel Junction to Undoped BaSi ₂ Overlayers. Japanese Journal of Applied Physics, 2012, 51, 04DP01.	1.5	1
502	Realization of Large-Domain Barium Disilicide Epitaxial Thin Film by Introduction of Miscut to Si(111) Substrate. Japanese Journal of Applied Physics, 2012, 51, 10NB06.	1.5	1
503	Enhanced photocarrier generation in large-scale photonic nanostructures fabricated from vertically aligned quantum dots. Optics Express, 2014, 22, A225-32.	3.4	1
504	Self-Modulating Incorporation of Sb in Si/SiGe Superlattices during Molecular Beam Epitaxial Growth.	0.3	0

14		acioni or oo in orforoo oupo
	Matoriala Science Forum	, 1993, 117-118, 159-164.
	ivialerials science rorum,	, 1993, 11/-110, 139-104.

#	Article	IF	CITATIONS
505	Physics and Control of Si/Ge Heterointerfaces. Materials Research Society Symposia Proceedings, 1996, 448, 125.	0.1	0
506	Exciton diffusion dynamics in quantum wells on a V-groove patterned Si substrate. Solid-State Electronics, 1996, 40, 733-736.	1.4	0
507	Exciton diffusion dynamics in quantum nanostructures on V-groove patterned substrates. Superlattices and Microstructures, 1998, 23, 395-400.	3.1	Ο
508	Photoluminescence from pure-Ge/pure-Si neighboring confinement structure. Journal of Vacuum Science & Technology an Official Journal of the American Vacuum Society B, Microelectronics Processing and Phenomena, 1998, 16, 1710.	1.6	0
509	Photoluminescence and Raman scattering of pure germanium/silicon short period superlattice. Acta Physica Sinica (overseas Edition), 1998, 7, 608-612.	0.1	0
510	Study of a Pure-Ge/Si Short-Period Superlattice by X-Ray Double Crystal Diffraction. Journal of Materials Synthesis and Processing, 1999, 7, 205-207.	0.3	0
511	Planarization of SiGe virtual substrates by CMP and its application to strained Si modulation-doped structures. , 0, , .		0
512	Grain growth of polycrystalline Si thin film for solar cells and its effect on crystal properties. , 0, , .		0
513	Si/multicrystalline-SiGe heterostructure as a candidate for solar cells with high conversion efficiency. , 0, , .		0
514	Growth of ZnO epitaxial films by metal organic chemical vapor deposition at various temperatures. , 0, , .		0
515	Fabrication of p-i-n Si/sub 0.5/Ge/sub 0.5/ photodetectors on SiGe-on-insulator substrates. , 0, , .		0
516	New solar cells using Ge dots embedded in Si PIN structures. , 0, , .		0
517	Investigation of crystal growth behavior of silicon melt for growing high quality polycrystalline silicon by cast method. , 0, , .		0
518	Evaluation of Strain Field Around SIC Particle in Poly-Crystalline Silicon. , 2006, , .		0
519	Spontaneous Modification of Grain Boundary Configuration and its Application for Realization of Bulk Multicrystalline Si with Electrically Inactive Grain Boundaries. , 2006, , .		0
520	Suppression of Structural Imperfection in Strained Si Thin Film by Utilizing SiGe Bulk Substrate. ECS Transactions, 2006, 3, 299-302.	0.5	0
521	ã,•āfªã,³āf³āfãf«ã,¯å\$çµæ™¶ã®ç²'界å^¶å¾¡ã«å'ã'ã┥. Materia Japan, 2006, 45, 720-724.	0.1	0
522	Annihilation of Acceptor–Hydrogen Pairs in Si Crystals Due to Electron Irradiation. Japanese Journal of Applied Physics, 2006, 45, 9162-9166.	1.5	0

#	Article	IF	CITATIONS
523	Two-dimensional Photonic Crystal Microcavity with Germanium Self-assembled Quantum Dots. , 2006, , .		0
524	Enhanced Light Emission from Ge Quantum Dots in Microdisks. Conference Proceedings - Lasers and Electro-Optics Society Annual Meeting-LEOS, 2007, , .	0.0	0
525	Hole density and strain dependencies of hole effective mass in compressively strained Ge channel structures. Physica E: Low-Dimensional Systems and Nanostructures, 2008, 40, 2122-2124.	2.7	0
526	Characterizations of polycrystalline SiGe films on SiO2 grown by gas-source molecular beam deposition. Thin Solid Films, 2008, 517, 254-256.	1.8	0
527	Functional Enhancement of Metal–Semiconductor–Metal Infrared Photodetectors on Heteroepitaxial SiGe-on-Si Using the Anodic Oxidation/Passivation Method. Japanese Journal of Applied Physics, 2008, 47, 2927-2931.	1.5	0
528	Current-injected light emitting device based on Si microdisk with Ge dots. , 2009, , .		0
529	Ge dots in Optical MicrocavitiesA Possible Direction for Silicon-based Light Emitting Devices. ECS Transactions, 2008, 16, 857-864.	0.5	0
530	Effect of reflected waves on the GISAXS analysis of as-grown capped Ge nanodots. Journal of Physics: Conference Series, 2009, 184, 012005.	0.4	0
531	Photoresponse properties of BaSi <inf>2</inf> films on N ⁺ -BaSi <inf>2</inf> /P ⁺ -Si tunnel junction for high efficiency thin film solar cells. , 2010, , .		0
532	Formation mechanism of twin boundaries in silicon multicrystals during crystal growth. , 2010, , .		0
533	Drastic reduction of crystallization time during Al-induced crystallizaion of amorphous Si by Ge adlayer. , 2011, , .		0
534	High efficiency quantum dot solar cells using 2-dimensional 6.4-nm-diameter Si nanodisk with SiC interlayer. , 2012, , .		0
535	Formation of polycrystalline silicon films with μm-order-long grains through liquid-phase explosive crystallization by flash lamp annealing. , 2012, , .		0
536	Improved internal quantum efficiency in high-quality BaSi <inf>2</inf> films grown by molecular beam epitaxy. , 2012, , .		0
537	Investigation of the carrier recombination process in undoped barium disilicide epitaxial films. , 2012, ,		0
538	Enhanced carrier extraction under strong light irradiation in Ge/Si type-II quantum dot solar cells. , 2012, , .		0
539	Effect of Ge/Si heterostructures on carrier extraction in Si solar cells with Ge quantum dots. , 2013, , \cdot		0
540	Characterization of grain boundary properties in BaSi2 epitaxial films on Si(111) and Si(001) by Kelvin probe force microscopy. , 2013, , .		0

#	Article	IF	CITATIONS
541	Improvement of excess-carrier lifetime in BaSi <inf>2</inf> epitaxial films by post-growth annealing. , 2013, , .		Ο
542	Formation of Uniaxially Strained Si/Ge Channels on SiGe Buffers Strain-Controlled with Selective Ion Implantation. ECS Transactions, 2013, 50, 815-820.	0.5	0
543	Effects of Annealing Process on the Structure of Mn-Doped BiFeO ₃ Thin Films. Key Engineering Materials, 0, 566, 155-158.	0.4	Ο
544	Enhanced p-type conductivity and band gap narrowing in heavily B-doped p-BaSi <inf>2</inf> films grown by molecular beam epitaxy. , 2013, , .		0
545	Effect of Ge/Al thickness on Al-induced crystallization of amorphous Ge layers on glass substrates. Physica Status Solidi C: Current Topics in Solid State Physics, 2013, 10, 1781-1784.	0.8	Ο
546	Electrical and optical characterizations of an n-BaSi <inf>2</inf> /p-Si hetero-junction for solar cell applications. , 2014, , .		0
547	Simulation study of Ge/Si heterostructure solar cells yielding improved open-circuit voltage and quantum efficiency. Japanese Journal of Applied Physics, 2014, 53, 110312.	1.5	Ο
548	Grain boundaries characterization of semiconducting BaSi <inf>2</inf> thin films on a polycrystalline Si substrate. , 2014, , .		0
549	Optical Properties of Quantum-Dot-Based Surface Photonic Nanostructures in Ge/Si Quantum Dot Solar Cells. , 2014, , .		Ο
550	Engineering of p-n junction for high efficiency semiconducting BaSi2 based thin film solar cells. , 2014, , .		0
551	Investigation of the cause of reduced open circuit voltage in Ge/Si quantum dot solar cells. , 2014, , .		0
552	Improvement of annealing procedure to suppress defect generation during impurity gettering in multicrystalline silicon for solar cells. , 2014, , .		0
553	Light trapping in large-scale photonic nanostructures fabricated from vertically aligned Ge quantum dots on crystalline silicon. , 2014, , .		0
554	Effect of miniband formation in a quantum dot super lattice fabricated by combination of bio-template and neutral beam etching for high efficiency quantum dot solar cells. , 2014, , .		0
555	Si-based new material for high-efficiency thin film solar cells. , 2014, , .		0
556	Structural control of dendrite crystals in practical size silicon ingots grown by floating cast method. , 2015, , .		0
557	Control of the electrical properties of BaSi <inf>2</inf> evaporated films for solar cell applications. , 2016, , .		0
558	Study on ion implantation conditions in fabricating compressively strained Si/relaxed Si 1â^'x C x heterostructures using the defect control by ion implantation technique. Journal of Crystal Growth, 2017, 468, 601-604.	1.5	0

#	Article	IF	CITATIONS
559	Thermal stability of compressively strained Si/relaxed Si 1-x C x heterostructures formed on Ar ion implanted Si (100) substrates. Materials Science in Semiconductor Processing, 2017, 70, 127-132.	4.0	Ο
560	Solar Cells Application of p-type poly-Si Thin Film by Aluminum Induced Crystallization. , 2017, , .		0
561	Overview of Surface Passivation Schemes for Thin Film Solar Cells. , 2017, , .		0
562	Fabrication of Cul/a-Si:H/c-Si Structure for Application to Hole-selective Contacts of Heterojunction Si Solar Cells. , 2017, , .		0
563	Local Structure of High Performance TiO <inf>x</inf> Passivating Layer Revealed by Electron Energy Loss Spectroscopy. , 2018, , .		Ο
564	Application of light trapping structure using Ge dot mask by alkaline etching to heterojunction solar cell. , 2018, , .		0
565	Development of the Passivation Layer For P-type Cul Thin Film Fabricated by the 2-step Method as the Novel Hole Selective Contact of Silicon Heterojunction Solar Cells. , 2018, , .		Ο
566	Significant improvement on electrical properties of BaSi2 due to atomic H passivation by radio-frequency plasma. , 2019, , .		0
567	Fabrication of Si1-xSnx Layer on Si Substrate by Screen-Printing of Al-Sn Paste. ECS Transactions, 2019, 93, 61-62.	0.5	Ο
568	Fabrication of group IV semiconductor alloys on Si substrate applying Al paste with screen-printing. Japanese Journal of Applied Physics, 2020, 59, SGGF07.	1.5	0
569	3D visualization of growth interfaces in cast Si ingot using inclusions distribution. Journal of Crystal Growth, 2020, 535, 125535.	1.5	Ο
570	(Invited) Application of Machine Learning for High-Performance Multicrystalline Materials. ECS Transactions, 2021, 102, 11-16.	0.5	0
571	Realization of the Crystalline Silicon Solar Cell Using Nanocrystalline Transport Path in Ultra-thin Dielectrics for Reinforced Passivating Contact. , 2021, , .		Ο
572	Versatile fabrication of a passivation material, solute PEDOT:PSS, for a c-Si substrate using alcoholic solvents. Sustainable Energy and Fuels, 2021, 5, 666-670.	4.9	0
573	Effect of Si diffusion on growth of GeSi self-assembled islands. Springer Proceedings in Physics, 2001, , 377-378.	0.2	0
574	Single and coupled quantum wells: SiGe. Landolt-Bâ^šâ^,rnstein - Group III Condensed Matter, 2007, , 26-49.	0.0	0
575	Geometry Control of Si-based Photonic Nanostructures Coupled with Quantum Dot Multilayers and Integration to Crystalline Si Solar Cells. , 2014, , .		0
576	Excitonic Band Edge Luminescence in Strained Si1-xGex/Si Quantum Well Structures Grown by Gas-Source Si Molecular Beam Epitaxy. , 1992, , .		0

#	Article	IF	CITATIONS
577	"Solid Source" Molecular Beam Epitaxial Growth of Highly Luminescent Si1-xGex/Si Quantum Well Structures. , 1992, , .		Ο
578	Anomalous spectral shift of photoluminescence from MBE-grown strained Si1â^'xGex/Si quantum wells mediated by atomic hydrogen. , 1996, , 36-39.		0
579	Intense photoluminescence from Si-based quantum well structures with neighboring confinement structure. , 1996, , 27-30.		0
580	Photoluminescence investigation on growth mode changeover of Ge on Si(100). , 1996, , 265-269.		0
581	SiGe Quantum Structures. Nanoscience and Technology, 1998, , 264-271.	1.5	Ο
582	Influence of surface roughness of ZnO layer on the growth of polycrystalline Si layer via aluminum-induced layer exchange process. Journal of Advanced Marine Engineering and Technology, 2016, 40, 692-697.	0.4	0
583	Electrical properties of TiO TiO _x bilayer prepared by atomic layer deposition at different temperatures. , 2019, , .		0
584	Work function of indium oxide thin films on p-type hydrogenated amorphous silicon. , 2020, , .		0
585	Structural properties of triple junctions acting as dislocation sources in high-performance Si ingots. , 2020, , .		0
586	Fabrication of silicon-nanocrystals-embedded silicon oxide passivating contacts. , 2020, , .		0
587	Fractal dimension analogous scale-invariant derivative of Hirsch's index. Applied Network Science, 2022–7	1.5	0